

“Babeş-Bolyai” University, Faculty of Physics, Cluj-Napoca, Romania
&
University of Osnabrück, Department of Physics, Germany

Cristina-Mihaela Gruian

**Protein adsorption onto bioactive glass –
conformational changes and quantitative analysis**

PhD Thesis

Summary

Scientific coordinators:

Prof. dr. Simon Simion

Prof. dr. Heinz-Jürgen Steinhoff

Cluj-Napoca

2011

Table of Contents

1. INTRODUCTION	1
2. MATERIALS AND METHODS	5
2.1 Sample preparations	5
2.1.1 Bioactive glass preparation	5
2.1.2 Spin labeling	5
2.1.3 Protein adsorption	5
2.2 Sample analysis	6
2.2.1 Cw-EPR measurements	6
2.2.2 Four pulse DEER measurements	6
2.2.3 FTIR measurements	7
2.2.4 XPS measurements	7
2.2.5 SEM measurements	7
3. RESULTS AND DISCUSSION	7
3.1 Horse methemoglobin	7
3.1.1 Immobilization of methemoglobin on the bioactive glass substrate	7
3.1.2 Conformational changes in methemoglobin structure, induced upon interaction with bioactive glass substrate – inter spin distances	9
3.1.3 Conformational changes in methemoglobin structure, induced upon interaction with bioactive glass substrate – secondary structure	11
3.1.4 Quantitative adsorption analysis	13
3.2 MnmE from <i>E.coli</i>	18
3.2.1 Immobilization of MnmE on the bioactive glass substrate	18
3.2.2 Conformational changes in MnmE structure, induced upon interaction with bioactive glass substrate – inter spin distances	21
3.2.3 Conformational changes in MnmE structure, induced upon interaction with bioactive glass substrate – secondary structure	25
3.2.4 Quantitative adsorption analysis	27
4. CONCLUSIONS	30
Selective Bibliography	32

Keywords: *protein adsorption, bioactive glass, spin labeling, EPR, horse methemoglobin, MnmE, FTIR, conformational changes, concentration of adsorbed protein, glutaraldehyde.*

1. Introduction and motivation

Protein adsorption and subsequent changes in their conformation are the first biomechanical events taking place at the surface of an implant after implantation and are determinants for further physicochemical interactions. Hence, the first step in evaluating the blood and tissue compatibility of any medical device is to study its behavior in terms of interactions with proteins. Both, the total amount of adsorbed protein as well as the overall protein-implant surface area interactions are of primary importance for the biocompatibility of a bioengineered material. Adsorption of protein molecules onto solid surfaces frequently results in conformational and/or orientational changes within the adsorbed layer [SERVAGENT-NOINVILLE *et al.* 2000, DOUSSEAU and PEZOLET 1990]. Because protein structures are relatively unstable, proteins tend to unfold, allowing internal regions to form additional contacts with a particular solid surface [EL-GHANNAM *et al.* 1999]. This denaturation is often associated with a loss of secondary or tertiary structure and results in irreversible adsorption.

Despite an increased understanding of many facets of protein adsorption in recent years, little is known about conformational changes in protein's structure. Moreover, protein behavior in its native environment after adsorption as well as details concerning protein dynamics and the exact amount of the protein attached remain largely unknown [LATOUR 2005, GRAY 2004, WERTZ and SANTORE 2001]. Most of the techniques which are frequently used to gain such information exhibit serious limitations and are not easily adaptable to proteins adsorbed on solid surfaces. For example, it is difficult to obtain high resolution X-ray structural information for the adsorbed proteins, whereas circular dichroism is not easily adaptable to proteins adsorbed on solid surfaces [KARLSSON *et al.* 2000, TIAN *et al.* 1998]. Although many studies have used Fourier Transform Infrared (FTIR) spectroscopy as a surface-sensitive technique to investigate protein structure, this method is not able to provide information about the protein dynamics or its tertiary structure. Besides the methods mentioned above, site-directed spin labeling (SDSL) in combination with Electron Paramagnetic Resonance (EPR) spectroscopy is a potent alternative, which provides both detailed structural and dynamic information [FANUCCI *et al.* 2003, HUBBELL *et al.* 2000], and therefore becomes very useful for the analysis of proteins in their native environment. SDSL involves the introduction of a spin label at a specific site in the amino acid sequence by cysteine substitution mutagenesis followed by modification of the sulfhydryl group with a nitroxide reagent.

Up to now, this method has been predominantly used for studying the structure and dynamic of soluble proteins in solution or membrane proteins reconstituted in their native membrane environment [BORDIGNON and STEINHOFF, 2007]. Only few studies reported recently that it can be extended to proteins adsorbed on planar lipid bilayers [JACOBSEN *et al.* 2005, RISSE *et al.* 2003], or even on quartz solid surface [JACOBSEN *et al.* 2006]. Nevertheless, in these studies only continuous wave EPR (cw-EPR) measurements are presented, to investigate adsorption-induced conformational changes at the level of the backbone fold.

A primary goal of this work is to use EPR spectroscopy combined with site-directed spin labeling for investigating adsorption of proteins on solid surfaces. In addition to cw-EPR, we intend to determine inter spin distances in proteins adsorbed on solid surfaces by means of double electron electron resonance (DEER) pulsed EPR from which a more detailed picture of the protein conformation and conformational changes can be deduced. Another aim of this study is to investigate the effect of glutaraldehyde as protein coupling agent in protein adsorption on bioactive glasses. For this purpose, interaction of two model proteins: horse methemoglobin and MnmE (*5-methyl-aminomethyl-uridine forming enzyme*) with bioactive glass which is commonly used as biomaterial for bone defects repair was investigated in terms of conformational changes and quantitative adsorption properties.

Both proteins are medium size (horse methemoglobin has a molecular mass of 66.5 kDa while MnmE is a 50 kDa protein) but belong to different classes. Horse methemoglobin is a metalloprotein consisting of four polypeptide chains: two alpha types (141aa each) and two beta types (146aa each). Each protein chain subunit contains a heme group whose four nitrogen atoms chelate an iron atom, but unlike hemoglobin, the iron is oxidized into Fe^{3+} , inhibiting the oxygen-binding capabilities of the protein. It is worth to mention here that previous studies have shown that GA induces polymerization of hemoglobin [MACDONALD and PEPPER 1994, OKUDA *et al.* 1991, GUILLOCHON *et al.* 1986, WEETALL 1974]. This protein has many lysine residues located on the surface, and interaction of these residues with GA leads to protein cross-linking [OKUDA *et al.* 1991, WEETALL 1974], resulting in a multitude of species, e.g. dimers, trimers and larger species [MACDONALD and PEPPER 1994, GUILLOCHON *et al.* 1986]. This heterogeneous mixture of hemoglobin products with a variety of molecular weights and chemical modifications makes the tetrameric structure of the molecule more rigid.

MnmE is a more complex protein, belonging to the class of G proteins. Previous studies have shown that G domains of MnmE is activated by dimerization [GASPER *et al.* 2009], displays lower affinities towards nucleotides and it requires GTP hydrolysis (stimulated by the presence of K^+ [SCRIMA and

WITTINGHOFFER 2006, SCRIMA *et al.* 2005]) to be functionally active. The crystal structure of MnmE dimer suggests that each monomer consists of three domains: an N-terminal domain responsible for constitutive dimerization, a central helical domain, and the G domain [SCRIMA *et al.* 2005]. It was already shown that in the nucleotide free state the G domains face each other with their nucleotide binding sites (Figure 2) without displaying any structural contacts between each other [MEYER *et al.* 2009]. In the presence of GDP-AlF_x, which is the transition state mimicking the GTP hydrolysis, the G domains contact each other by overcoming a 20-30 Å distance gap [BOEHME *et al.* 2010a, BOEHME *et al.* 2010b]. This large conformational change occurring upon activation makes this protein ideally suited to study the influence of protein-bioactive glass interaction on functional conformational dynamics.

For elucidation of structural changes which may occur upon adsorption of horse methemoglobin and MnmE on the surface of bioactive glasses, both proteins were investigated by EPR spectroscopy, in terms of spin label side chain dynamics and inter spin distances. In this regard, paramagnetic centers were introduced in special locations in both proteins. Thereby, native cysteine from position β-93 in horse methemoglobin was spin-labeled with (4-(2-Iodoacetamido)-2,2,6,6-tetramethyl-1-piperidinyloxy) spin label (Figure 1).

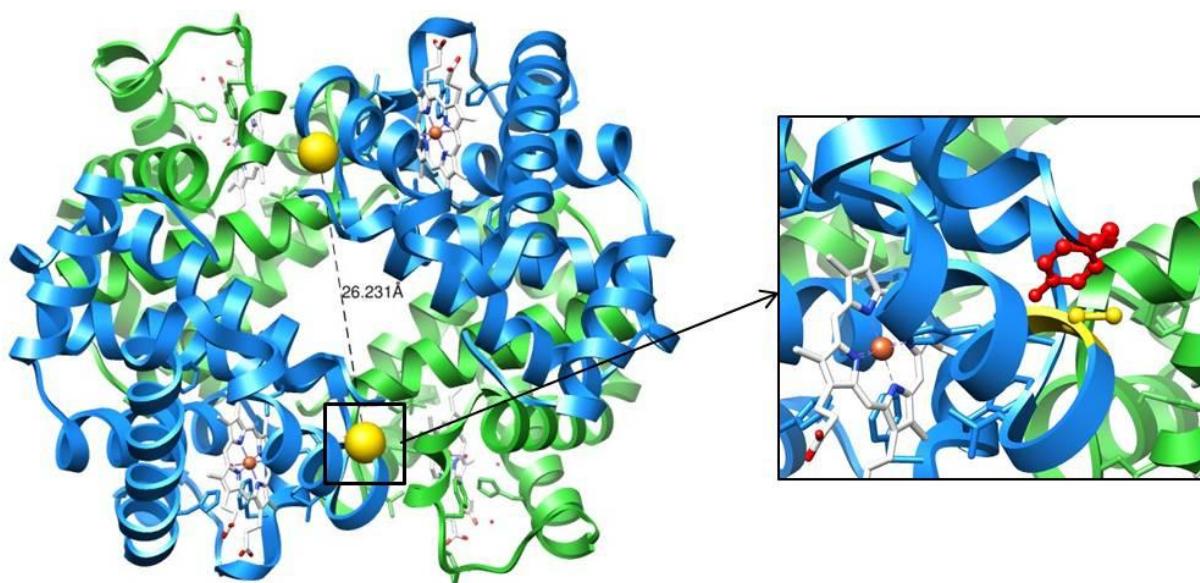


Figure 1 Left: Structure of methemoglobin obtained by X-ray crystallography (2ZLU from Protein Data Bank). The α -chains are colored in green and the β -chains are colored in blue; heme groups are shown in stick representation. The C $_{\beta}$ atoms of native cysteines from position β -93 are indicated as yellow spheres, with dashed lines showing distance between the C $_{\beta}$ atoms of both residues. **Right:** Detailed view into the spin label binding site. The native amino acid at position β -93(cysteine) is colored in yellow and the tyrosine situated in a pocket close to the C-terminus of the β -chain is colored in red

In the case of MnmE, four positions were mutated to cysteine and then spin labeled with (1-oxy-2,2,5,5-tetramethyl-3-pyrroline-3-methyl) methanethiosulfonate spin label (MTSSL): Ser278 and Glu287 (both in the G-domain) and Ile105 and Lys95 (situated in the N terminal domain of the protein) (Figure 2). These locations were chosen to provide information on the position of the two monomers relative to each other in both open (apo) and closed (GDP·AlF_x) state when the protein is adsorbed on the bioactive glass.

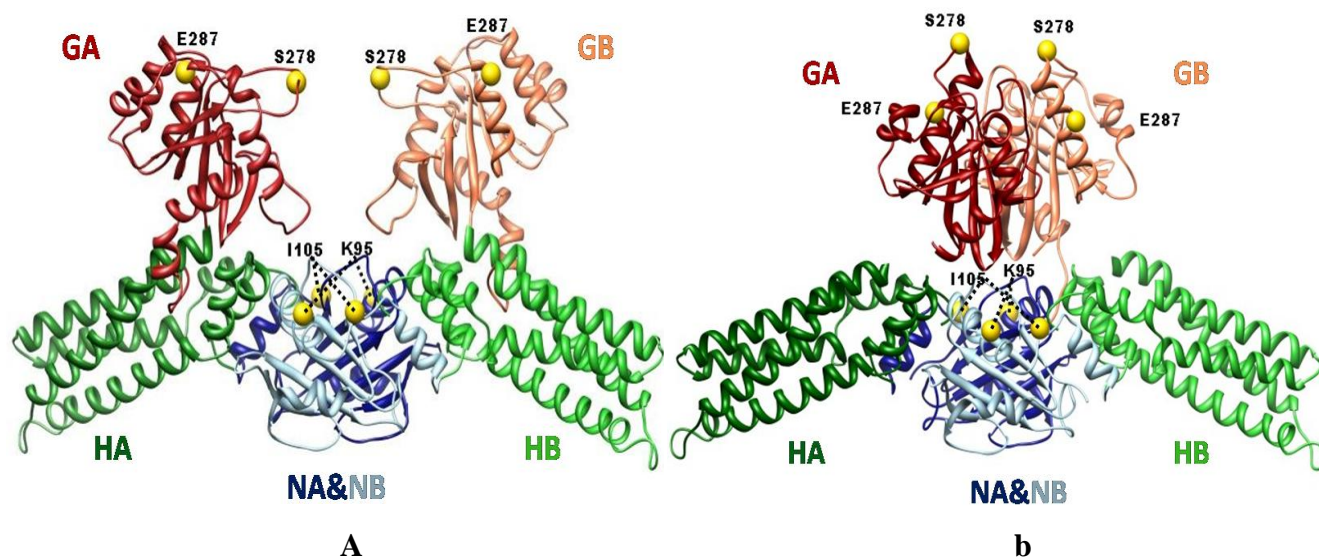


Figure 2. MnmE Mutants. Positions of native residues that were mutated to cysteines and spin labeled are indicated by yellow spheres. (a) Open conformation of the MnmE protein generated with pdb 1XZP; (b) Closed conformation of the G domains [pdb 2GJ8] superimposed on the TmMnmE crystal structure. Domains are labeled as follows: N-terminal domains (NA, NB), α -helical domains (HA, HB) and G-domains (GA,GB).

Also, the properties of an implant material are influenced by the secondary structure of the protein in its adsorbed state. Hence, we have addressed the study of both proteins and their changes in secondary structure upon adsorption by means of FTIR spectroscopy. Besides the information about the protein conformation after adsorption, the amount of the protein adsorbed on the surface is of great importance for the properties of an implant material. In this regard, concentration of protein attached on bioactive glass was determined by means of EPR and FTIR spectroscopies. X-Ray Photoelectron spectroscopy (XPS) was used to follow the chemical modification of the outermost few nanometers layer of the bioactive glass (BG) surface, in order to analyze the surface coverage. Moreover, the surface morphology of bioactive glass was analyzed before and after protein adsorption by Scanning Electron Microscopy (SEM).

2. Materials and Methods

2.1. Sample preparation

2.1.1. Bioactive glass preparation

The bioactive glass (BG) system used as substrate for protein attachment was prepared by the sol-gel method [HENCH and WEST 1990] and is identical in composition with the classical 45S5 Bioglass[®]: 45% SiO₂, 24.5% Na₂O, 24.5% CaO and 6% P₂O₅ (in molar %). After preparation, the bioactive glass was milled and the particle size of the obtained powder ranged from hundreds of nm to few μm. The water contact angle recorded on the BG surface before milling was 41°, indicating a hydrophobic character of the BG surface after preparation [VERNE *et al.* 2009, TUNC *et al.* 2005]. In order to facilitate protein adsorption, the surface of bioactive glass was silanized with 3-aminopropyl-triethoxysilane (APTS) and subsequently modified with glutaraldehyde (GA) [CHEN *et al.* 2007, CHEN *et al.* 2006, WILLIAMS and BLANCH 1994].

2.1.2. Spin labeling

Horse methemoglobin. The native cysteine at position β-93 in horse methemoglobin was labeled with (4-(2-Iodoacetamido)-2,2,6,6-tetramethyl-1-piperidinyloxy) spin label using the following protocol: oxyhemoglobin was extracted from fresh horse blood samples according to Benesch *et al.* (1972) and then converted to methemoglobin by the addition of a 2-fold amount of K₃Fe(CN)₆ [STEINHOFF *et al.* 1989]. Spin labeling of the methemoglobin with (4-(2-Iodoacetamido)-2,2,6,6-tetramethyl-1-piperidinyloxy) followed the procedure of McCalley *et al.* (1972). Labeling efficiencies were determined to be 80%.

MnmE from E. coli. Purified, nucleotide-free Cys-mutants of *E. coli* MnmE: Glu287, Ser278, Ile105 and Lys95, were pretreated with dithioerythritol (DTE, 4°C, 2 hours) to reduce any disulfides to thiols. After removal of DTE via filtration, the protein solutions were incubated with 1 – 5 mM (1-oxy-2,2,5,5-tetramethylpyrroline-3-methyl)methanethio-sulfonate spin label (MTSSL, Toronto Research; Alexis Biochemicals) for 16 hours at 4°C. Unbound MTSSL was removed by gel filtration.

2.1.3 Protein adsorption

Horse methemoglobin. Powder samples were incubated for 4 hours at room temperature (298 K) in a solution of 150 mg/ml (≈2 mM) horse methemoglobin in phosphate buffer (0.01M, pH 7.4).

MnmE from E.coli. Powder samples were incubated for 4 hours at room temperature (298 K) in a solution with a protein concentration of 10-25 mg/ml (200-500μM). Buffer conditions were 100 mM

KCl, 50 mM Tris-DCl (pH 7.5), 5mM MgCl₂ in D₂O. In order to obtain the transition state analog GDP-AlF_x, 200-400 μM of nucleotide-free Mn²⁺ already adsorbed on the BG substrate were incubated in 1 mM GDP, 1 mM AlCl₃ and 4 mM NaF.

All samples were stored for 30 days at 4°C in eppendorf tubes and then ultrasonicated for 45 minutes at room temperature. After ultrasonication, the samples were washed three times with buffer solution to remove the protein that was probably detached from the surface during the process. Finally, the samples were transferred to EPR capillaries and measured at room temperature to verify the stability of protein attachment.

2.2. Sample analysis

2.2.1. Cw-EPR measurements

X band cw-EPR experiments were performed using a homemade EPR spectrometer equipped with a Bruker dielectric resonator. The microwave power was set to 1.0 mW; the B-field modulation amplitude was 0.15 mT. Sample volumes greater than 15 μl (the bioactive glass volume) were filled into EPR glass capillaries with 0.9 mm inner diameter (the EPR-active volume of the sample tube was 10 μl).

Concentration of protein adsorbed on the bioactive glass was estimated by calculating the area of EPR absorption spectrum, which is directly proportional to the spin concentration in the sample. The protein concentration was calculated by comparison of this area with the one of a reference spin probe of known concentration (2,2,6,6-tetramethyl-1-piperidinyloxy (TEMPO)).

2.2.2. Four pulse DEER measurements

Pulse EPR measurements were carried out at X-band frequencies (9.3-9.4 GHz) with a Bruker Elexsys 580 spectrometer equipped with a Bruker Flexline split-ring resonator ER 4118XMS3 and a continuous flow helium cryostat (ESR900, Oxford Instruments) controlled by an Oxford Intelligent temperature controller ITC 503S. Prior to freezing the protein in 3mm inner diameter EPR tubes, the samples were supplemented with 10% (by volume) glycerol for horse methemoglobin and 12.5% (by volume) glycerol for Mn²⁺. The measurements were performed using the four-pulse DEER sequence [PANNIER *et al.* 2000]:

The total measurement time for each sample was 4÷48 h. Background correction and determination of interspin distance distributions were carried out using the program DEERAnalysis (2010) and a

model of randomly oriented spins with respect to the dipolar axis and Tikhonov regularization [JESCHKE *et al.* 2006].

2.2.3. FTIR measurements

FTIR spectroscopic analyses were performed in reflection configuration with a JASCO 6200 FTIR spectrometer in the 4000 to 400 cm^{-1} spectral domain with a resolution of 4 cm^{-1} . Gaussian peak analysis of the amide I band was performed to analyze the secondary structure of the proteins before and after adsorption on bioactive glass. Peak locations were determined by second derivative analysis [DONG *et al.* 1990, BYLER and SUSI 1986] and correlated with values found in previous studies [KONG and YU 2007, NATALELLO *et al.* 2005, ARRONDO and GONI 1999, SESHADRI *et al.* 1999, SUSI and BYLER 1983]. The amount of adsorbed protein was estimated by the peak area ratio of amide I to amide II, according to the findings of Buchanan and El-Ghannam (2010).

2.2.4. XPS measurements

The XPS measurements carried out to analyze the surface functionalization of bioactive glass microparticles with protein were performed using an SPECS PHOIBOS 150 MCD system equipped with monochromatic $\text{AlK}\alpha$ source (250 W, $h\nu = 1486.6$ eV), a hemispherical analyzer and a multichannel detector. The curve-fitting analysis of N 1s was performed by using Gaussian curve fitting function in the CasaXPS software.

2.2.5. SEM measurements

SEM images were recorded using FEI Quanta 3D FEG 200/600 Scanning Electron Microscope. The sample powders were covered with platinum (Pt) in order to amplify the secondary electrons signal. This coating was performed in an Agar Automatic Sputter Coater at standard atmospheric pressure (1013 mBar).

3. Results and Discussion

3.1. Horse methemoglobin

3.1.1. Immobilization of methemoglobin on the BG substrate

For the spin-labeled side chains that are exposed to solution the nitroxide mobility refers to rotational correlation times of the nitroxide in the ns time range. This in turn results in EPR spectra characterized by narrow line widths of the center lines and small apparent hyperfine splitting. If the mobility of the spin label side chain is restricted by interactions with neighboring side chains or surfaces, the line widths

and the apparent hyperfine splitting are increased [KLARE and STEINHOFF 2009]. At first glance, the X band cw-EPR spectrum of methemoglobin in solution (Figure 3a) is the sum of two components. Such multicomponent spectra are referred to as “complex” and can be associated with two possible situations: (1) a conformational exchange between two states of the protein [BRIDGES *et al.* 2010], so that in an equilibrium mixture, with slow exchange between states, the spectrum is a sum of two components in proportion to their populations; (2) a rotameric equilibrium, which explains the line shape as the result of the side chain existing in multiple rotameric states. However, the presence of an isosbestic point for methemoglobin in solution, at approximately 3432 G field value (determined from X-band cw-EPR measurements in the temperature range from 5 to 25 degrees Celsius (Figure 3b) suggests that in this case the origin of the complex spectrum is the equilibrium of the JAA side-chain between two states with different mobility. This assessment is in agreement with the Moffat’s interpretation [MOFFAT 1971], who attributed the components related to the mobile (α) and immobile (β) fractions of the spin label side chain to different orientations of the spin labels with respect to the protein. One of these orientations is free in solution on the surface of the molecule and the other is strongly immobilized, corresponding to the spin labels which occupy the tyrosine pocket, Tyr HC₂(145) β in the C-terminus of the β -chain (Figure 1) [MOFFAT 1971].

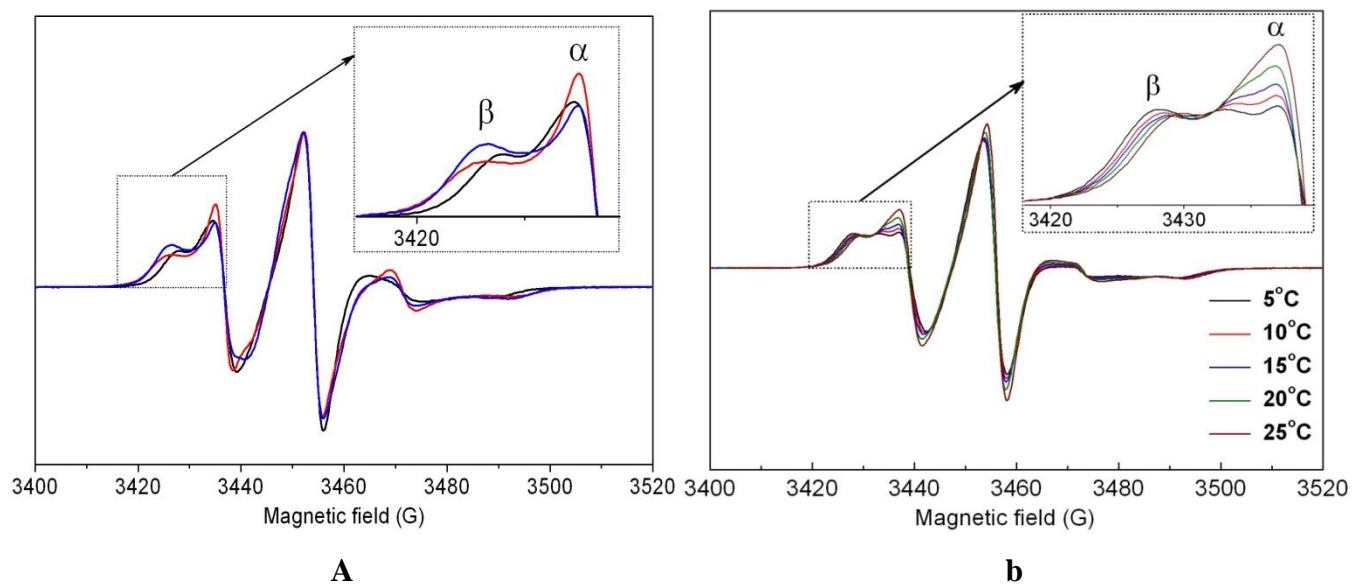


Figure 3 (a) Room temperature X-band cw-EPR spectra of horse methemoglobin spin-labeled in position β -93* recorded in solution (black) and in adsorbed state immediately after immersion on bioactive glass without GA (red) and with GA (blue). Inset: The mobile and immobile components visible in the lower field spectral lines are depicted with α and β , respectively. (b) X-band cw-EPR spectra recorded for methemoglobin in solution, in the temperature range from 5 to 25 degrees Celsius. Inset: the mobile and immobile components visible in the lower field spectral lines are denoted as α and β respectively.

Upon protein adsorption on bioactive glass, the equilibrium between the two conformations is significantly shifted towards the component β (Figure 3a). This indicates that the spin labels interact with the BG surface or with adjacent domains of protein. A notable feature is the increase of the line width observed for the immobile component after adsorption (see the inset of Figure 3a), that cannot be associated only with the spin labels that are trapped into the tyrosine pocket. This line broadening can be explained by assuming that the movement of the entire protein molecule is restricted due to interaction with bioactive glass.

To further address the influence of GA on nitroxide mobility when the protein is attached to the BG substrate, the spin label mobility was analyzed in terms of fractions of populations, reorientational correlation times and the semiempirical mobility parameter (the inverse of the central resonance line width). When the protein is attached on the BG without GA treatment all the above parameters indicate higher degree of motional freedom for the spin labels oriented to the protein surface. This suggests that the structure in the vicinity of position β -93 is changed upon adsorption in a way which would allow for a fraction of spin labels to avoid the tyrosine pocket and to rotate less restricted than in solution. Giving the fact that position β -93 is located in an α -helical domain, one possible explanation would be that part of this helix unfolds upon adsorption and, consequently, motion of the spin label which point to the protein surface is less restricted compared to the same spin label attached to MetHb in solution. On the other hand, when the BG substrate is functionalized with GA, restrictions in spin label mobility are more pronounced, suggesting that the protein molecule becomes more rigid as a consequence of the polymerization induced by the protein coupling agent [MACDONALD and PEPPER 1994, GUILLOCHON *et al.* 1986, WEETALL 1974].

3.1.2. Conformational changes in methemoglobin structure, induced upon interaction with BG substrate – inter spin distances

SDSL-EPR in combination with DEER spectroscopy was applied to determine intramolecular distances between the two β -93 positions in methemoglobin before and after adsorption on bioactive glass. The C_{β} - C_{β} distance between the two β -93 positions in methemoglobin determined from X-ray structure is 26.23 Å for the protein in its native state (Figure 1). A recent study reported a distance of about 25.3 Å between the two positions β -93 of human hemoglobin labeled with MTS [BANHAM *et al.* 2007]. Our DEER measurements revealed a distance of 24.8 Å between the β -93 sites of methemoglobin

in solution (Figure 4), which is in agreement with the distance of 25.3 Å presented by Banham and coworkers. The small difference in the determined distance appears because we used a spin label (JAA SL) with a slightly longer side-chain than MTS.

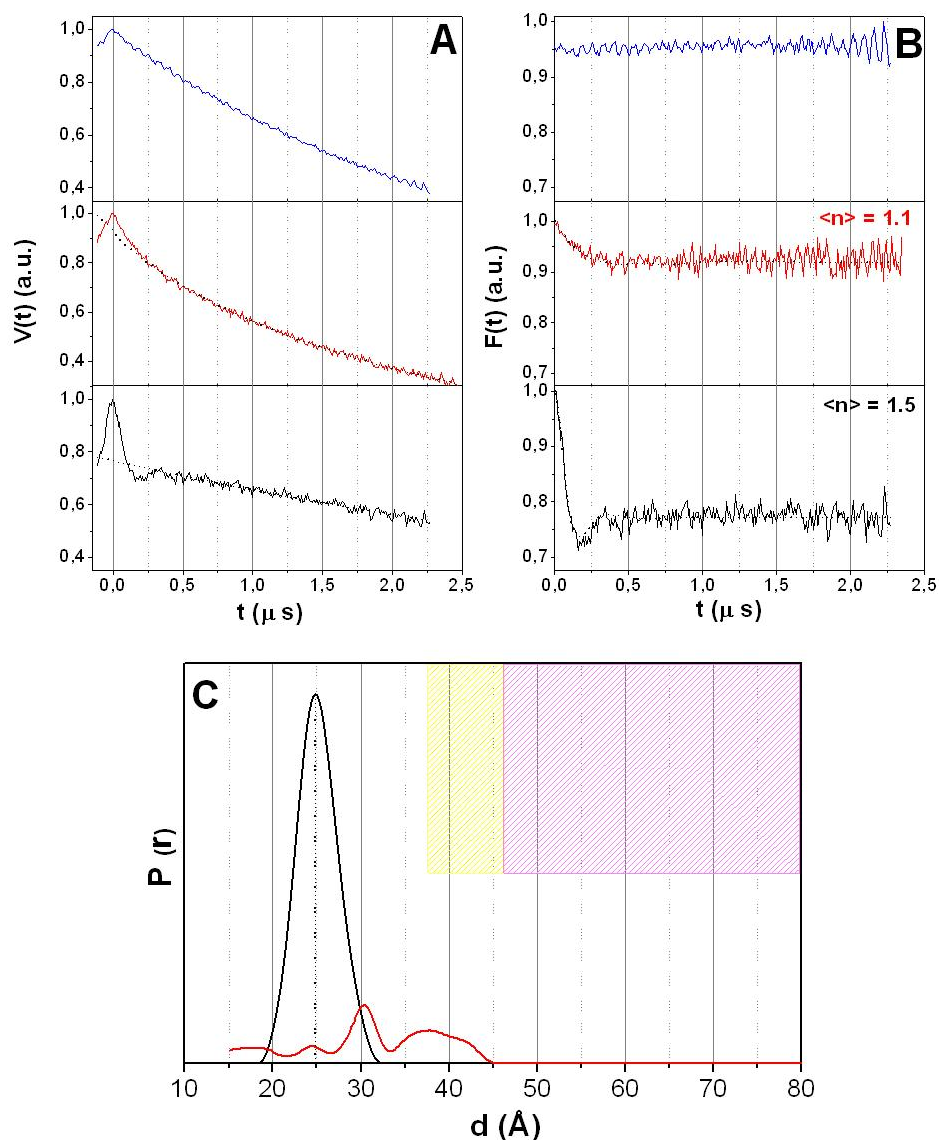


Figure 4 DEER characterization of horse methemoglobin spin labeled in position β -93: **(A)** dipolar evolution function not corrected for background; **(B)** background corrected dipolar evolution data; **(C)** distance distributions obtained by Tikhonov regularization. Black dotted lines in the panels (A) and (B) are fits to the data obtained by Tikhonov regularization. The black lines correspond to the spectra recorded in solution, while the red and blue lines represent the spectra recorded in adsorbed state on BG without GA and with GA treatment, respectively. Calculated spin numbers per complex ($\langle n \rangle$) are depicted. Colored boxes show the reliability of the distance data: white = reliable distance and distribution; light yellow = approximate distance but no information about the distribution; light magenta = no predictions possible.

A qualitative evaluation of the DEER traces recorded after adsorption can be directly derived by eye from the form factor $F(t)$ extracted from dipolar evolution function $V(t)$ [POLYHACH and JESCHKE 2007]. A first observation is that all DEER spectra recorded in adsorbed state have a very low modulation depth (<0.1 in case of BG without GA and 0 for BG treated with GA), pointing out that a very small number of spins have dipolar-dipolar interaction (Figure 4). We assume that the low number of pairs of interacting spins is caused by protein dissociation. In fact, it was shown that hemoglobin dissociates at extreme pH values (below 4 and above 10), upon addition of detergents or at low concentrations [PIN and ROYER 1994, VALDES and ACKERS 1977]. Moreover, taking into account that the subunits of hemoglobin are to a large extent held together by hydrophobic interactions [ANTONINI and BRUNORI 1971], it is likely that the interaction between the hydrophobic surface of bioactive glass and the protein molecules results in dissociation and denaturation.

DEER experiments conducted with methemoglobin attached on BG without GA treatment have shown that a small fraction of protein keeps its tetrameric structure upon adsorption, in this case allowing us to obtain a distance distribution (Figure 4). However, intensity of the distance distribution curve is much lower than for the protein in solution as a consequence of the reduced number of spins pairs with distances between 2÷8 nm.

Distance distributions obtained after the analysis using Tikhonov regularization showed that when the protein is attached on the BG the distance between the two β -93 positions is bigger than for the protein in solution (Figure 4). This leads to the assumption that the two β chains are slightly apart for the protein in adsorbed state compared to the protein in solution. Projected on the protein, this means that in adsorbed state the tetrameric structure adopts a conformation that is slightly unfolded as a consequence of interaction between protein and BG surface.

Samples containing methemoglobin adsorbed on bioactive glass treated with GA represent a special case due to the total absence of modulation depth in the 4-pulse DEER data. We assume that the main factor contributing to this situation is polymerization of methemoglobin (and consequently a homogeneous spatial distribution of spin labels in the sample), due to the presence of GA.

3.1.3. Conformational changes in methemoglobin structure, induced upon interaction with BG substrate – secondary structure

Both amide I (centered at 1650 cm^{-1}) and amide II (centered at 1550 cm^{-1}) bands can be seen in the absorption profiles of methemoglobin after adsorption. To obtain information about conformational

changes which may appear in protein secondary structure upon adsorption we focused on the signal characteristic to amide I functional group.

Hemoglobin is an α -helical protein (86 % helix, according to X-ray crystallography) and contains no β -sheets [CAI and SINGH 2004]. The small peaks at ca. 1627 and 1695 cm^{-1} can therefore be assigned to the short loops connecting the helical cylinders [SUSI and BYLER 1983] and the pronounced peak between 1654–1656 cm^{-1} can be associated with α -helices (Figure 5). Contributions of β -turns are visible in the peak at about 1679–1682 cm^{-1} while the small peak at 1648 cm^{-1} is assigned to a random structure. The percentage of α -helix (74%) determined from the amide I region for lyophilized methemoglobin (Table 1) is in agreement with the values presented in previous FTIR studies [CAI and SINGH 2004, LUO *et al.* 1994].

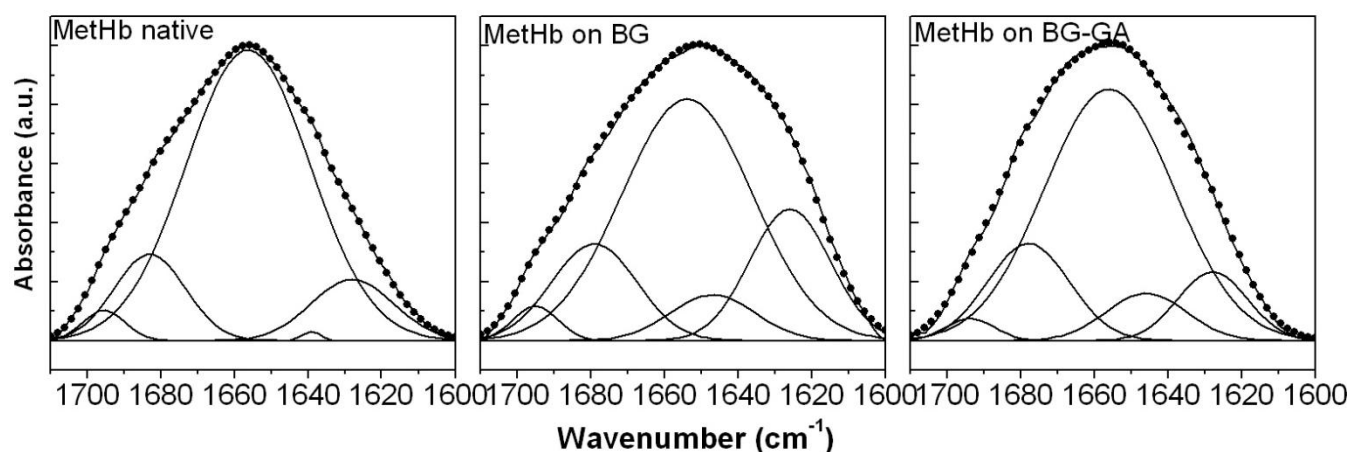
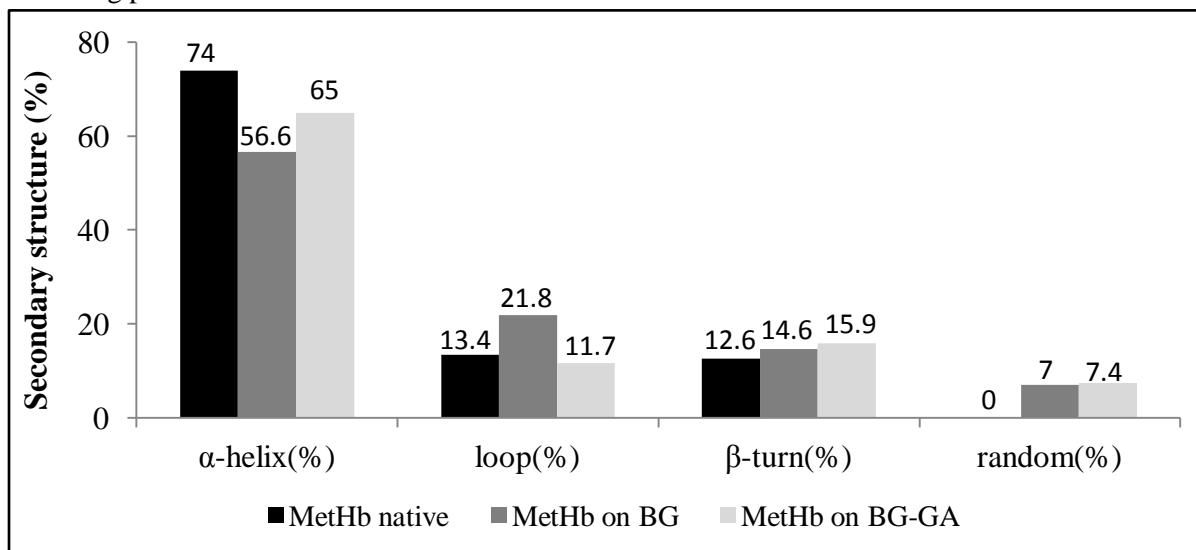


Figure 5 Separation of the amide I band into its components for horse methemoglobin before and after adsorption on BG without and with GA. The closed circles represent the sum of the separated band components. The errors are $\pm 1 \text{ cm}^{-1}$ for the band positions and $\pm 5\%$ for the peak areas.

Curve fitting analysis of amide I (Figure 5) reveals that on the BG surface, methemoglobin loses a large percentage of its α -helical structure (approximately 18 %), shown by a decrease in the percent area of the component band centered at 1654 cm^{-1} and a concurrent increase in β -turns, loops or random structure component (Table 1). This behavior suggests that the protein is somewhat denatured upon interaction with the BG surface, losing a large fraction of its helical secondary structure. This change in conformation may arise from a stronger interaction with the bioactive glass surface, a feature that has been previously reported for other proteins on this type of substrate [CHEN *et al.* 2007, CHEN *et al.* 2006, GRUIAN *et al.* 2011a, GRUIAN *et al.* 2011b, BUCHANAN and EL-GHANNAM 2010]. The unfolding of approximately 18% of α -helices upon adsorption correlated with the results obtained by cw-EPR

spectroscopy supports the assumption that the α helix, where position β -93 is located, unfolds upon adsorption.

Table 1 Distribution of secondary structure elements in methemoglobin. The uncertainty due to experimental error and fitting procedure are within the limit of ± 4 %



As a protein coupling agent, it is expected that glutaraldehyde maintains almost completely the native protein structure [HEULE *et al.* 2003, WILLIAMS and BLANCH 1994, WEETALL 1985]. Indeed, the deconvolution of amide I band (Figure 5) revealed that methemoglobin loses a smaller percentage of α -helix structure (approximately 11 %) when the bioactive glass is treated with glutaraldehyde (Table 1), confirming that the stability towards denaturation is higher on this substrate. However, the increase in the amount of disordered structures (β -turn and random) towards more stable elements like α -helices implies a certain denaturation of methemoglobin even when the bioactive glass is functionalized with glutaraldehyde. Therefore, we can assume that methemoglobin adsorption implies strong interactions with the BG surface, which in turn can disrupt the hydrogen bonds involved in stabilization of α -helices located at the outer parts of the protein.

3.1.4. Quantitative adsorption analysis

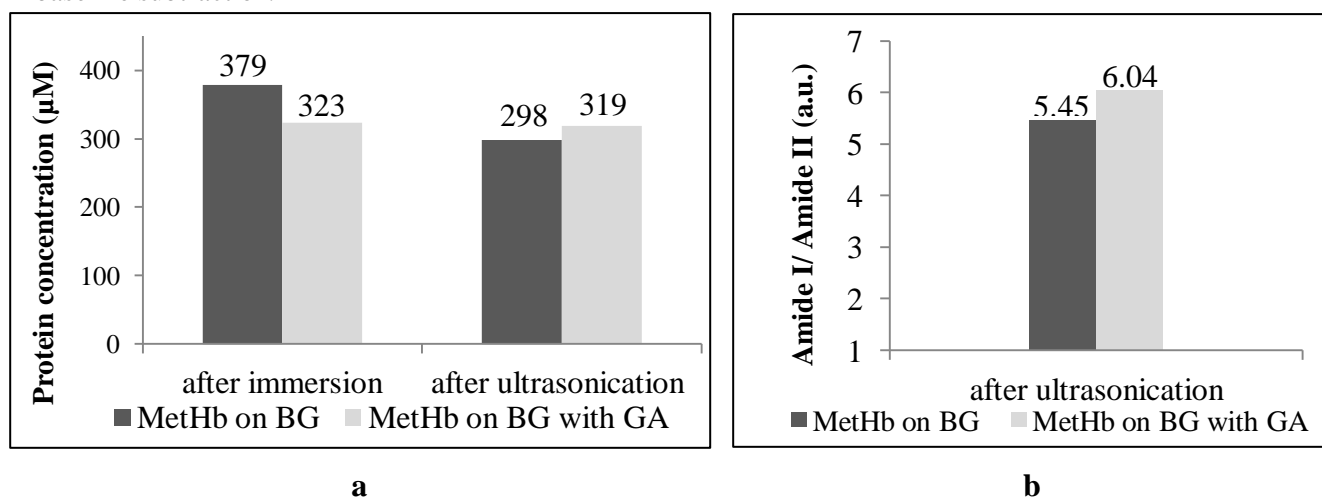
The amount of protein attached on BG was determined by means of three different spectroscopic techniques: EPR, FTIR and XPS spectroscopy. First, the amount of the protein attached to the bioactive glass was estimated from the value of spin concentration in the sample, which was calculated from the area of cw-EPR spectra recorded at room temperature. Certainly, in order to determine the real protein

concentration (not only the one which contains spin labels) the spin label efficiency had to be considered for these calculations.

Table 2a shows the amount of protein attached to the bioactive glass immediately after immersion as well as 30 days later and after ultrasonication. Immediately after immersion the protein shows greater affinity for BG without GA. Nevertheless, the EPR spectra recorded 30-days after incubation at 4°C in sample buffer as well as after 30 min of ultrasonication and subsequent washing steps indicated that a larger amount of protein is irreversibly bound in case of the bioactive glass treated with GA.

A second approach was to evaluate the amount of protein that remained on the BG surface after ultrasonication from the peak area ratio of amide I to amide II of FTIR spectra. This procedure allows us only to establish a comparison between amounts of protein attached on different substrates but it is not possible to determine the actual concentration of the adsorbed protein. Thereby, the results obtained by FTIR spectroscopy for protein concentration on BG substrates after ultrasonication (Table 2b) are in agreement with the results obtained by EPR spectroscopy for the same samples (Table 2a).

Table 2 (a) Molar concentration (in μM) of methemoglobin adsorbed on BG before and after ultrasonication. **(b)** Amide I/ Amide II ratio of intensities from FTIR spectra recorded for methemoglobin attached on BG after ultrasonication. For both methods, errors are estimated to $\pm 10\%$, due to experimental procedure and uncertainties in baseline subtraction.



X-ray photoelectron spectroscopy (XPS) [MUIR *et al.* 2008, BROWNE *et al.* 2004] was further used to analyze the protein coverage of the BG surface (were analyzed only the ultrasonicated samples). Protein adsorption was evidenced by using the 400 eV peak for N1s, the source of which could only be the protein (Figure 6).

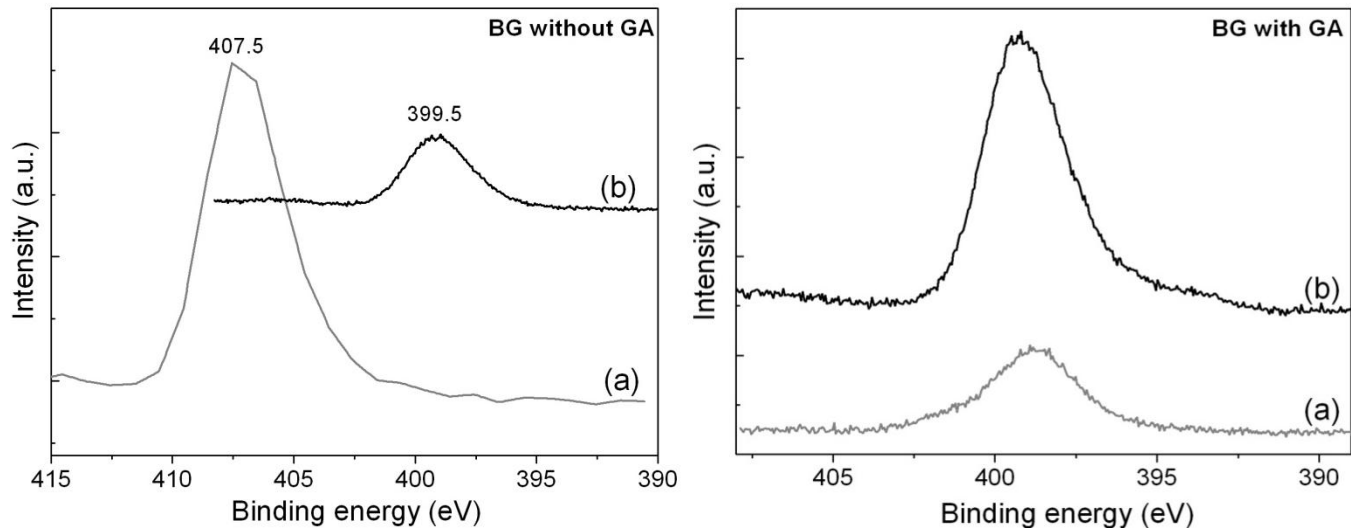


Figure 6 N 1s high resolution spectra of bioactive glass before (gray-a) and after immersion in horse methemoglobin solution (black -b). (the N 1s peak recorded at 407.5 eV does not contain contributions associated to organic matrixes; therefore, a high resolution spectra was not needed in this situation, the peak was subtracted from survey spectrum of BG without GA)

Although the BG system contains nitrogen, the N 1s photoelectron peak observed before immersion in protein solution is centered around 408 eV (Figure 6). This peak is typical for nitrogen in nitrates and appears as consequence of nitrates precursors used in bioactive glass preparation. After the treatment of BG with glutaraldehyde, the N 1s photoelectron peak from 408 eV disappears due to dissolution of nitrates during washing steps and a new peak appears at binding energy close to 400 eV, corresponding to N from amino group in 3-aminopropyl-triethoxysilane. Nevertheless, after immersion in protein solutions, the deconvolution of N 1s core level spectra reveals the presence of two components centered at 398.2 and 400 eV (Figure 7). Both components are characteristic to C-NH₂ bonds, but the latter one was found to be typical for nitrogen in organic matrix [VANEJA and SIMON 2011, SERRO *et al.* 2006]. Therefore, the intensity of this peak was considered marker for protein attachment (Table 3). The relative intensities of the N 1s XPS peak recorded around 400 eV for both BG substrates before and after immersion in protein solution (Table 3) show that more protein is attached on the substrate with GA treatment.

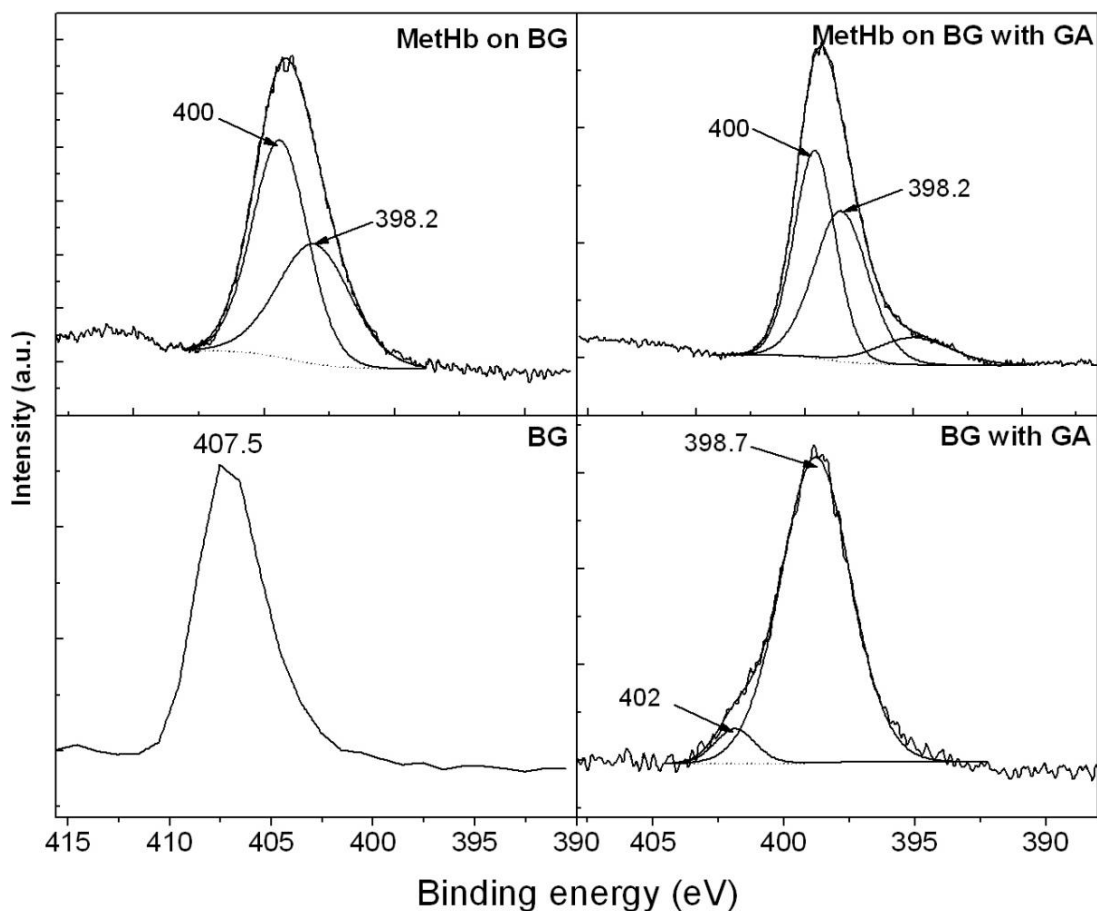
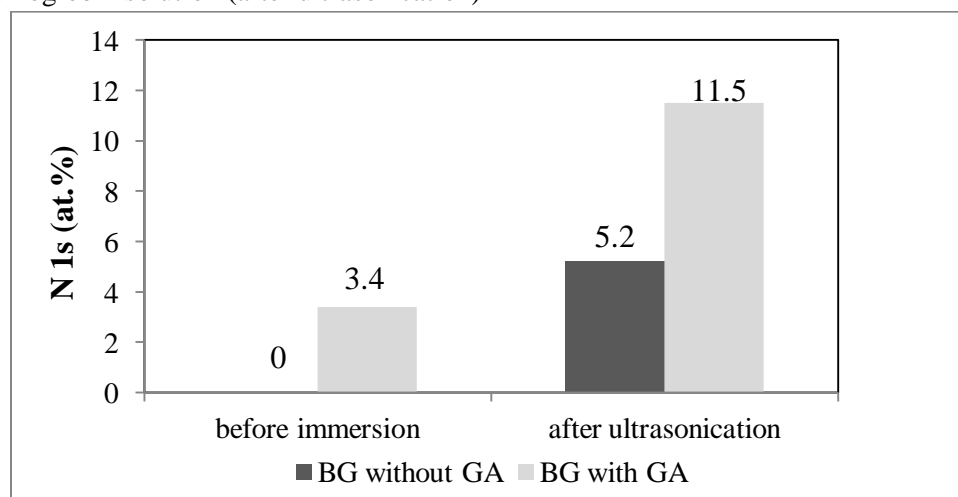


Figure 7 Deconvoluted N 1s high resolution XPS spectra of bioactive glass before and after immersion in horse methemoglobin solution. The N 1s peak recorded for BG at 407.5 eV does not contain contributions associated to organic matrixes; therefore, a deconvolution of this peak was not of interest for the purpose of this study.

Table 3 N1s atomic percentage on BG surface for the peak recorded around 400 eV before and after immersion in horse methemoglobin solution (after ultrasonication)



Taken together, all three techniques have shown that glutaraldehyde positively influences the protein binding stability on bioactive glass. We assume that in the presence of glutaraldehyde protein distribution on the BG surface is more organized; hence, the number of molecules having weak attachment points is much lower compared to the substrate which does not contain GA. This assumption is supported by the results from SEM characterization of both BG surfaces before and after immersion in protein solution (Figure 8 and Figure 9). When the BG substrate is treated with glutaraldehyde more regular organization of the protein layer can be observed (Figure 9). The chains that are observed on the surface of BG treated with GA have approximately 50 nm width, which would correspond to a macromolecule formed by 8-10 proteins. This interpretation further supports the hypothesis of protein polymerization and is supported by other studies which have shown that glutaraldehyde leads to the cross-linking of hemoglobin [WEETALL 1974] and resulting in formation of macromolecules consisting of 8-10 proteins [MACDONALD and PEPPER 1994, GUILLOCHON *et al.* 1986].

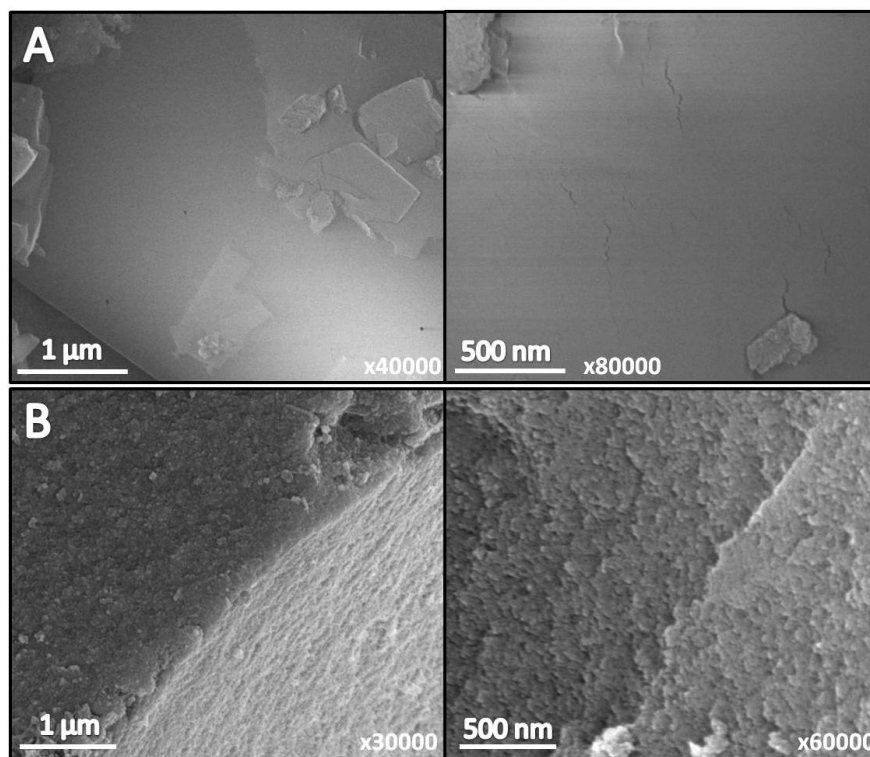


Figure 8 SEM images of BG without GA before (A) and after immersion in methemoglobin solution (B). The images in the right are recorded with a higher magnification. After adsorption a uniform layer of protein covers the BG surface.

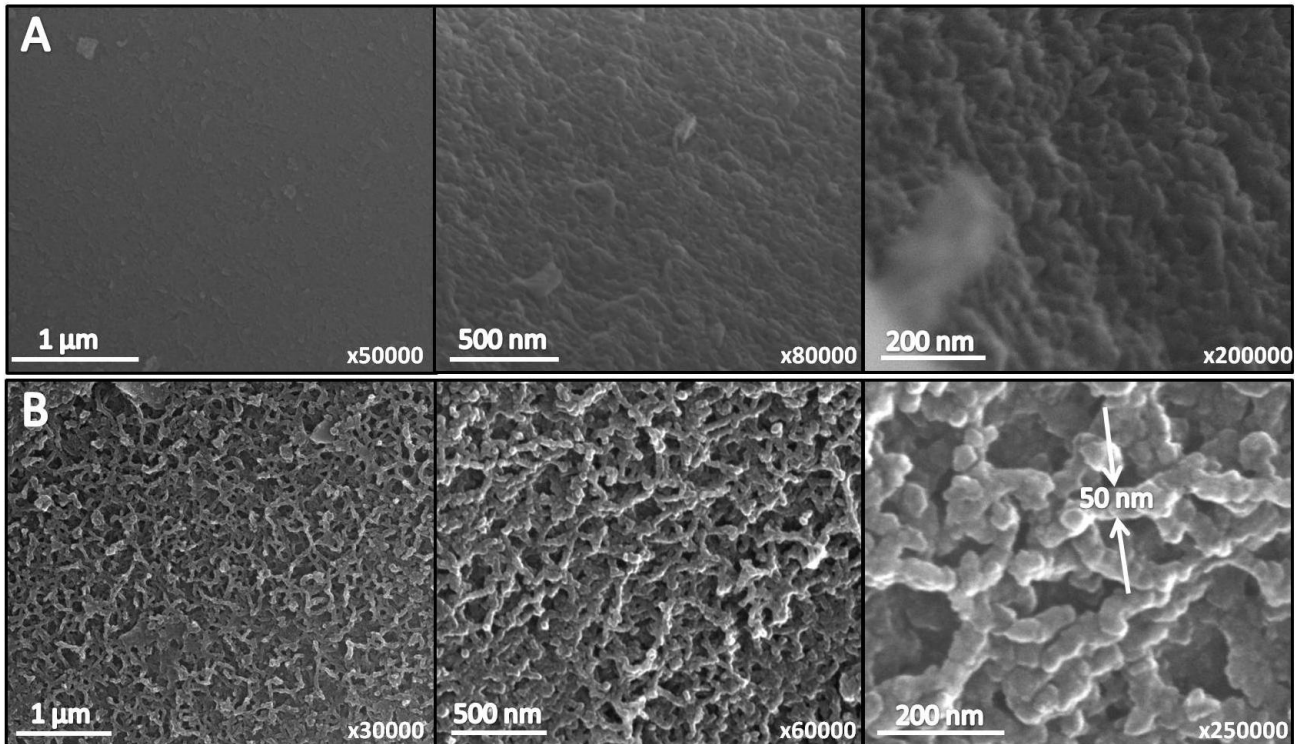


Figure 9 SEM images of the BG with GA, before (A) and after immersion in methemoglobin solution (B). The images in the center and right panels are recorded with higher magnification. Higher porosity can be observed on sample treated with GA, which is thought to be the result of microporosity induced by ion leaching during heat-treatment in water at 80°C.

3.2. *MnmE* from *E.coli*

3.2.1. Immobilization of *MnmE* on the BG substrate

In order to gain detailed information about the putative immobilization of the protein upon the adsorption onto BG, room temperature cw EPR measurements were performed for *MnmE* spin labeled in positions Ser278, Glu287, Ile105 and Lys95 (further on will be denoted as S278, E287, I105 and K95) (Figure 2).

Room temperature cw EPR spectra of *MnmE* in solution spin labeled in all four positions are characterized by the presence of two distinct components, related to the mobile (α) and immobile (β) fractions of the spin label side chain (Figure 10). The immobile component arises from a fraction of spin labels engaged in secondary and tertiary interactions which restricts their reorientational freedom. The mobile component can be assigned to the spin labels which have less constraints in their environment. Also, this component is influenced by general backbone fluctuations. Free unbound spin label exhibits

sharp resonance lines that superimposed the recorded spectra for positions E287, I105 and K95 (marked with a star symbol (*), Figure 10).

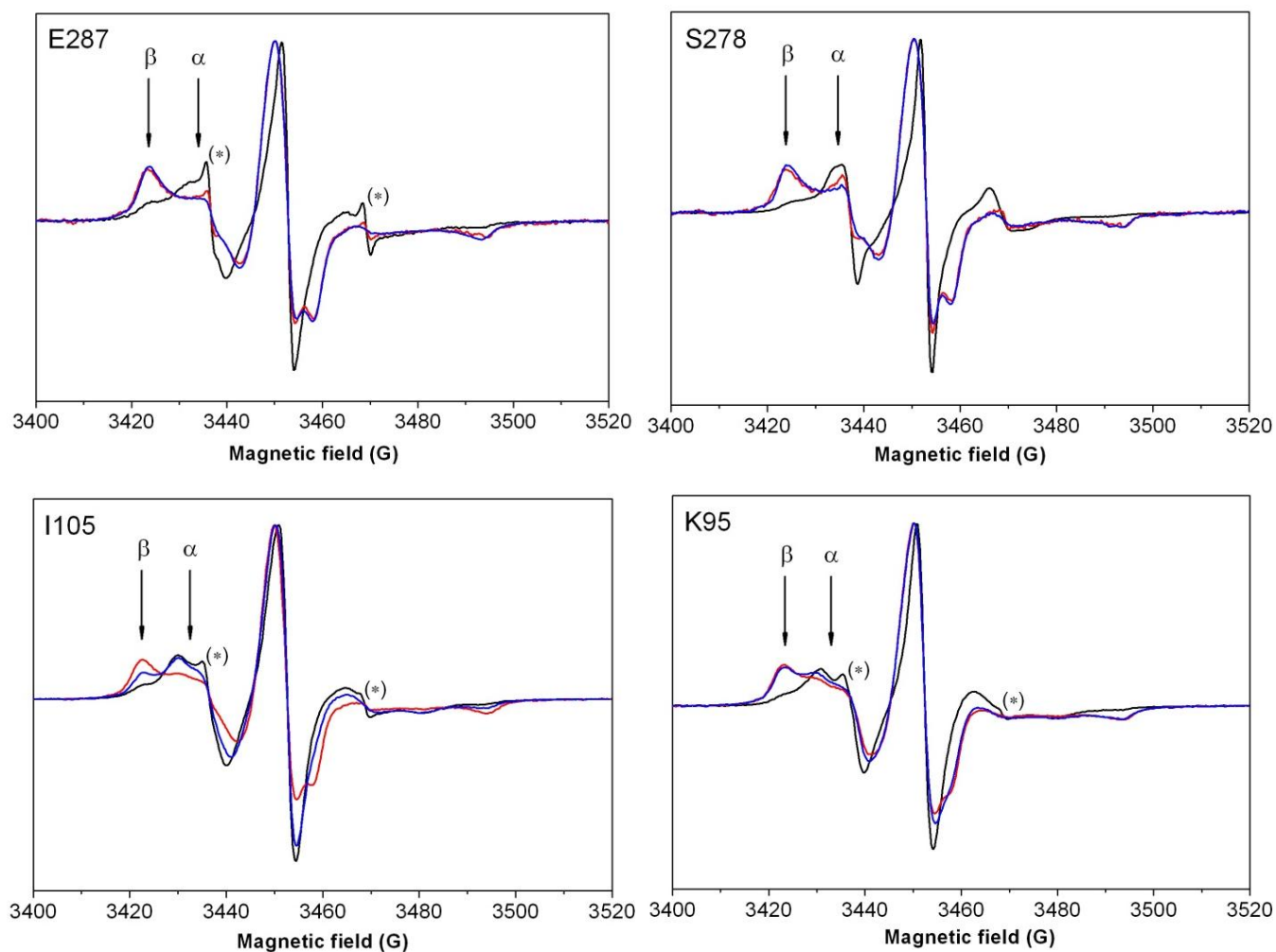


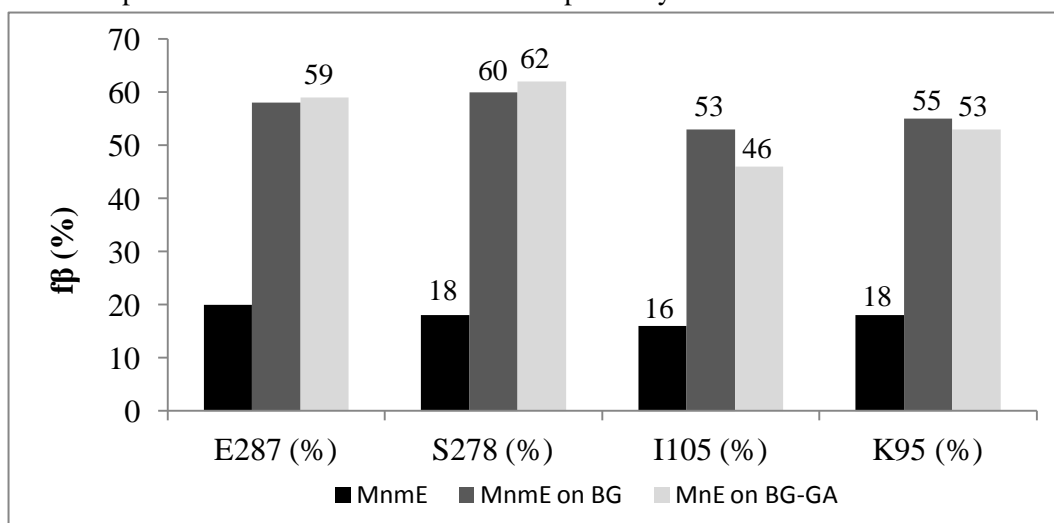
Figure 10 Room temperature cw-EPR spectra of the spin labeled MnME cysteine mutants E287, S278, I105 and K95 in solution (black lines) and in adsorbed state (red lines: on BG without GA, blue lines: on BG with GA). Shown are the spectra for open G-domain conformation (apo state). The mobile and immobile components are indicated by arrows α and β respectively. The peak marked by star symbol (*) corresponds to free unbound spin label in solution.

In solution all four positions exhibit a more pronounced mobile component. In the case of E287 this denotes a certain motional flexibility of the spin label side chain close to the top of the G-domain, while for S278 the higher mobile component is explainable by the location of this position in the loop region of switch II, which exhibits a very high structural flexibility. For the two positions situated in the N-

terminal domain of the protein, the mobile component is explainable by the deviations of both N-terminal domains in solution.

Upon adsorption, all spectra exhibit an increase in the width of the central resonance line and larger low field amplitude, suggesting that the spin label mobility is significantly decreased due to immobilization of the protein on the BG substrate. The amount of signal corresponding to immobile component was quantified by spectra simulations and expressed in terms of fraction of immobilized spin labels. Accordingly, protein immobilization is also reflected in the values obtained for the fraction of immobile component for each position before and after adsorption (these values are listed in Table 4).

Table 4 Fractions of immobile component determined from simulations of EPR spectra recorded for MnmE before and after adsorption on BG without and with GA respectively.



As can be seen in Figure 10 and Table 4, the most pronounced changes in side-chain dynamics upon adsorption on the bioactive glass appear for positions E287 and S278 situated in the G-domain of MnmE. This strong immobilization induced by adsorption on bioactive glass might be due to a direct interaction of this region with the BG surface, suggesting that these two positions may be close to contact points of the protein on the surface.

Effect of glutaraldehyde. According to X-ray crystallographic structure of MnmE [SCRIMA *et al.* 2005], this protein doesn't have many lysines at the surface as compared to hemoglobin. Thus, it is unlikely that interaction with GA would induce its polymerization. Although we expected a stronger attachment of the MnmE on the BG substrate after addition of the protein coupling agent, cw-EPR spectra revealed that mobility changes induced by functionalization with GA are quite small, except from position I105 at the N-terminal domain. In the case of the two positions situated in the G-domain (E287 and S278), the

use of glutaraldehyde leads to a very small increase of the immobile component, i.e. to a stronger attachment of this region of the protein on the BG surface. Although this behavior was expected, the differences which appear due to functionalization with GA are very small (1 ÷ 2 % in terms of fraction of immobilized spin labels). This might be due to the fact that the immobilization of this area on the BG substrate was already extremely pronounced without glutaraldehyde addition. Hence, these data support the assumption that these two positions are close to the contact points of the protein on the BG surface.

3.2.2. Conformational changes in MnmE structure, induced upon interaction with BG substrate – inter spin distances

As in the case of methemoglobin after adsorption on the bioactive glass, the main characteristic for all DEER traces is the low modulation depth of the signal (<0.1). Moreover, no modulation depth could be observed in case of protein adsorbed on BG without GA treatment. So no distance distribution could be obtained (Figures 11 and Figure 12).

The reasons which can cause this very low modulation depth were already discussed in Section 3.1.2. Accordingly, in case of MnmE we assume that the explanation for this situation is the dissociation of the protein and, consequently, distances higher than 8 nm between intramolecular spin labels. However, DEER traces for the spin labeled protein attached to the BG with GA showed a distinct modulation depth, allowing us to obtain a distance distribution. It seems that in this case, in contrast to the respective data obtained from hemoglobin, GA does not induce the polymerization of the protein due to the poor presence of lysines at the protein surface. This hypothesis is also supported by the SEM images (see Section 3.2.4), which do not show the formation of long protein chains like in the case of methemoglobin. Previous studies have shown that the protein coupling agent helps in maintaining the native protein structure upon adsorption [HEULE *et al.* 2003]. This might be a possible explanation for the fact that a small fraction of protein still keeps its dimeric form after adsorption on BG treated with GA.

A special case which must be discussed here is mutant S278: spin labels attached to this position seem to be too far apart from each other to be measurable within the sensitivity range of four DEER spectroscopy (a very low modulation depth was obtained when the protein is attached on both types of BG substrates) (Figure 11). The location of position 278 in the loop region of the G domain allows for a high flexibility which can explain the fact that the two spin labels are separated with a distance higher than 8 nm during adsorption of the protein on the BG. In solution, position S278 displays a major contribution (about 80 % from the distance distribution – average value calculated from the area under

the distance distribution curve) given by the spin labels which display a distance of 49 Å between them. After adsorption, the dissociation of the protein could lead to an increase of the interspin distance greater than 30 Å. This in turn might be too far apart to be detected by our experimental DEER setup.

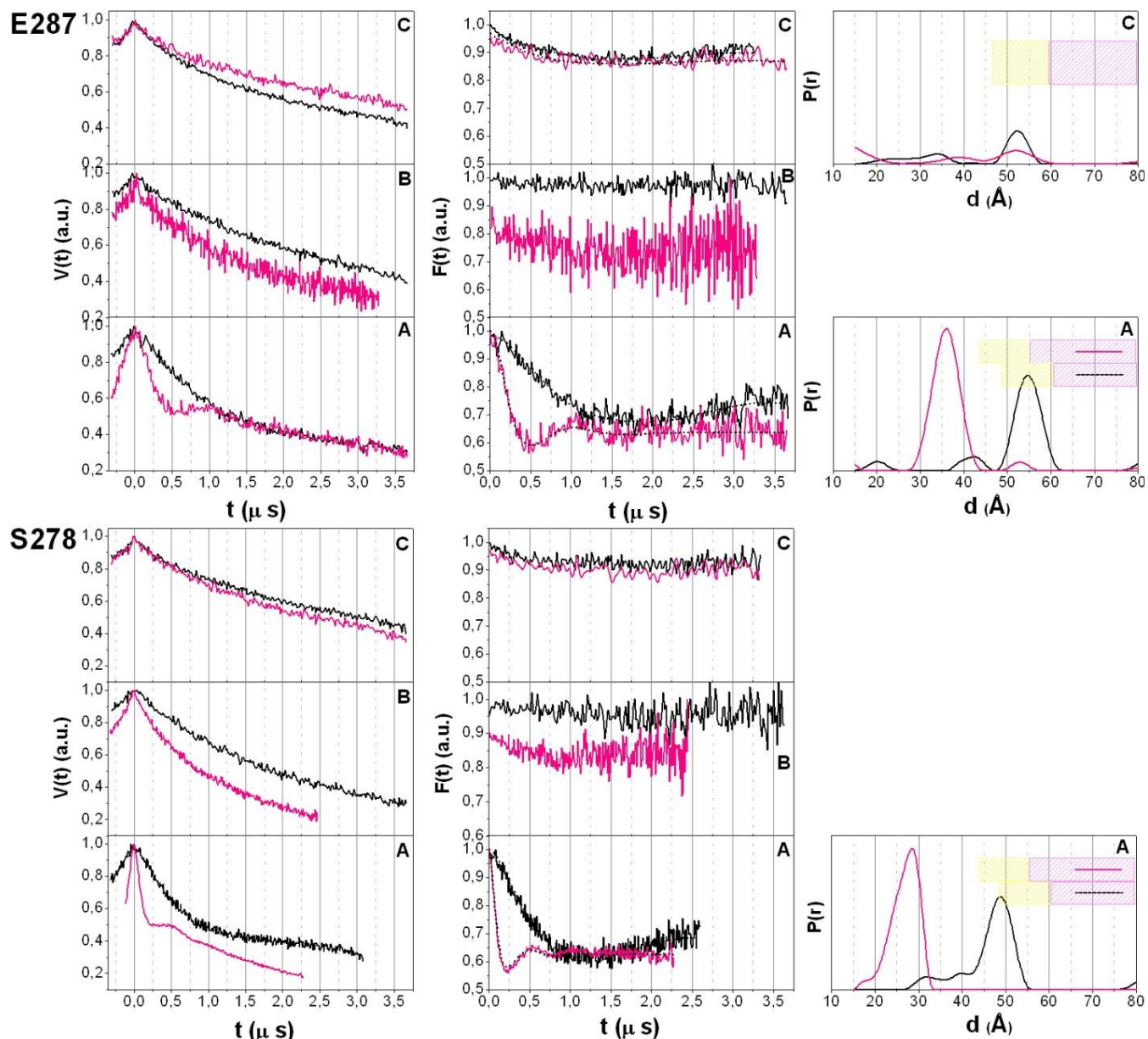


Figure 11 DEER comparison of MnmE mutants E287 and S278 in apo (black lines) and GDP·AlF_x (pink lines) state: left panel – dipolar evolution function not corrected for background; central panel – background corrected dipolar evolution data; right panel – distance distributions obtained by Tikhonov regularization. Dotted lines in the center panel are fits to the data obtained by Tikhonov regularization. Spectra recorded before and after adsorption on the BG without and with glutaraldehyde are shown in panels A, B and C respectively. Colored boxes show the reliability of the distance data: white = reliable distance and distribution; light yellow = approximate distance but no information about the distribution; light magenta = no predictions possible.

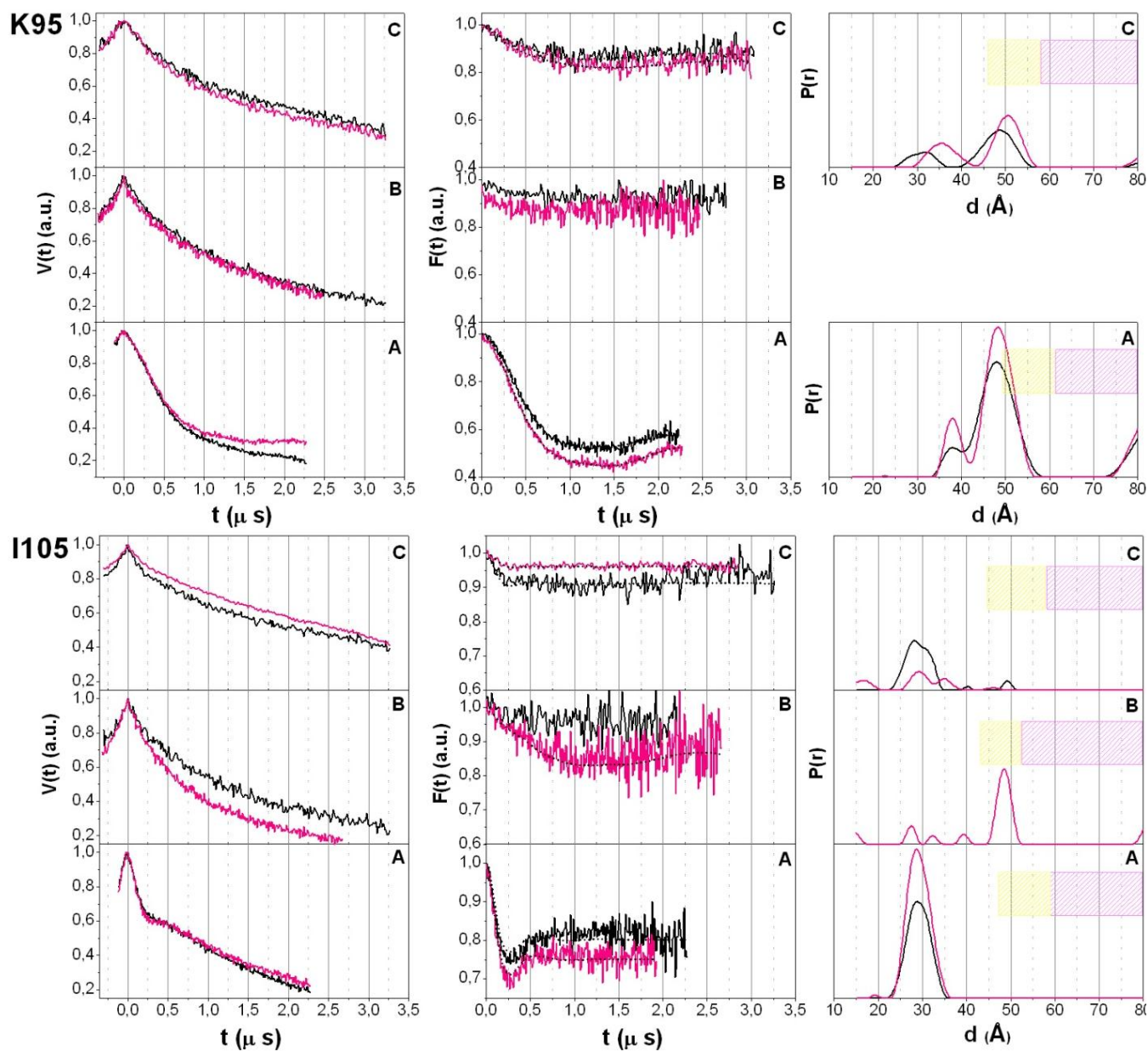


Figure 12 DEER comparison of MnmE mutants K95 and I105 in apo (black lines) and GDP-AIF_x (pink lines) state: left panel – dipolar evolution function not corrected for background; central panel – background corrected dipolar evolution data; right panel – distance distributions obtained by Tikhonov regularization. All plots are normalized by amplitude. Dotted lines in the center panel are fits to the data obtained by Tikhonov regularization. Spectra recorded before and after adsorption on the BG without and with glutaraldehyde are shown in panels A, B and C respectively. Colored boxes show the reliability of the distance data: white = reliable distance and distribution; light yellow = approximate distance but no information about the distribution; light magenta = no predictions possible.

Characterization of MnmE G domain mobility The conformational changes of MnmE that it undergoes during its GTPase cycle were previously studied by Meyer *et al.* (2009) by pulse double electron-electron resonance (DEER) spectroscopy. As mentioned in Section 1, the G domains face each

other in the nucleotide free state, but upon addition of GDP·AlF_x they overcome a 20-30 Å distance gap [MEYER *et al.* 2009, BOEHME 2010, SCRIMA and WITTINGHOFFER 2006] (see Figure 2).

However, after adsorption the major maxima recorded for positions E287 and S278 in transition state (GDP·AlF_x) are similar to those obtained for apo state (Figure 11), suggesting that the G domains of the protein remain in the open conformation. This result supports the hypothesis highlighted by the cw measurements, namely that after adsorption the protein “freezes” in open state, due to its immobilization on the solid surface.

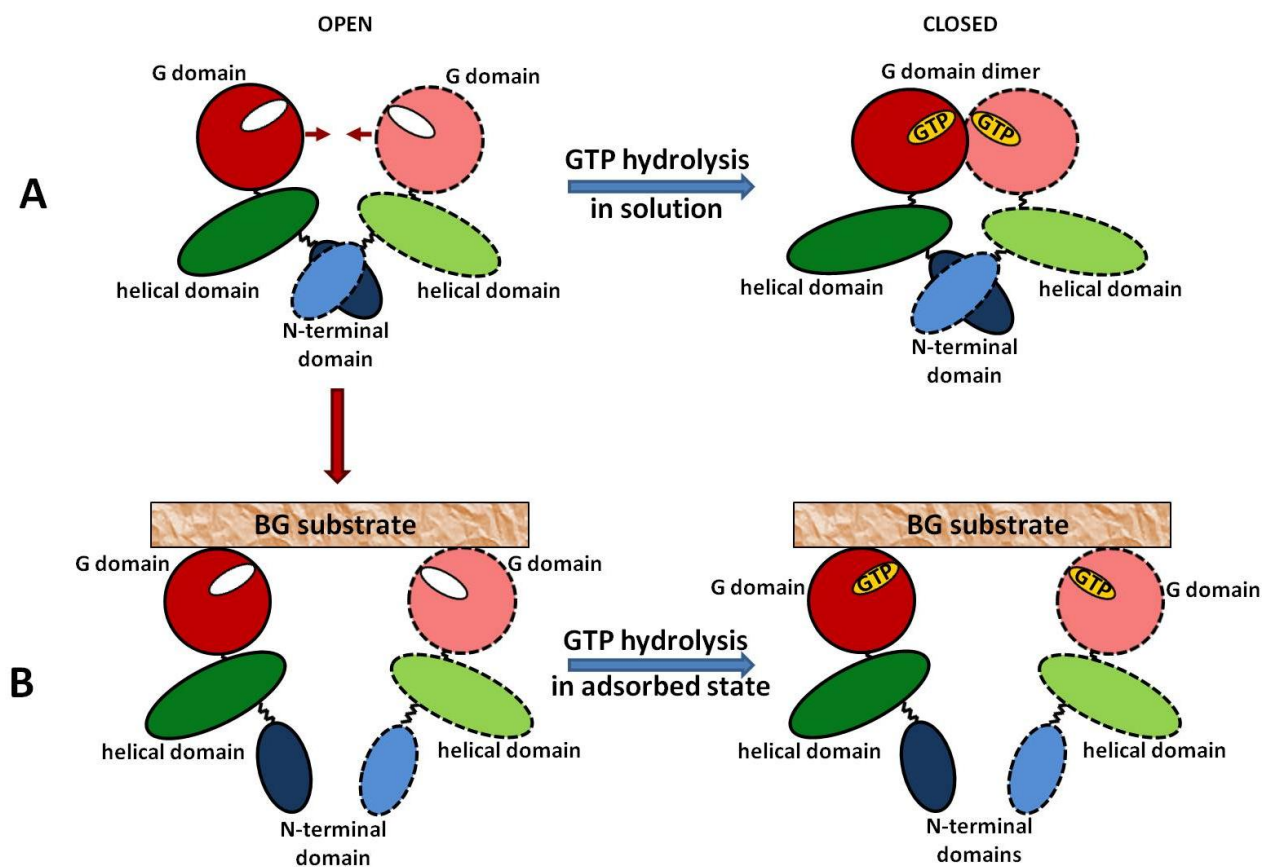


Figure 13 Schematic illustration of activation of MnME during GTP hydrolysis in solution and after adsorption on the bioactive glass. **A.** In solution, the G domains adopt an open conformation (in apo state) and a closed conformation (in transition state); **B.** Upon adsorption, the G-domains are the contact region with the BG substrate and, consequently, remain open in transition state. Figure adapted from [SCRIMA and WITTINGHOFFER 2006].

Furthermore, the major contributions obtained for positions I105 and K95 when the protein is adsorbed on BG with GA are similar with those obtained for the protein in solution: 48 Å (for K95) and 29 Å (for I105) (Figure 12). Yet, position I105 was the only sample with protein adsorbed on the BG

without GA, which displayed a modulation depth high enough to obtain a distance distribution with a maximum of 48 Å (20 Å longer than in solution or in case of BG with GA). This increase of distance between these two positions (which implies a separation of the two N-terminal domains) explains the increase of spin label mobility when the protein is adsorbed on BG without GA and supports the idea that the protein dissociates upon adsorption on BG in the two constitutive monomers (see Figure 13).

3.2.3. Conformational changes in methemoglobin structure, induced upon interaction with BG substrate – secondary structure

The deconvolution of amide I into its components shows that there are several conformational changes for the protein adsorbed on both types of surfaces (Figure 14). It is worth to mention here that the solvent used for this protein was D₂O (see Section 2.1). So, the assignment of peak locations to secondary structure elements was done accordingly). For instance, the major band at 1657.5 cm⁻¹, assigned to the α-helix structures of the protein is slightly shifted after adsorption (1659 cm⁻¹) (Table 5). The higher band position at 1659 cm⁻¹ corresponds to weaker hydrogen bonding, leading to more flexible helices [TATULIAN 2001]; we assume that this difference in the helix flexibility appears as consequence of interaction between the protein and bioactive glass.

Table 5 Assignments of amide I frequencies to secondary structure elements for MnmE before and after adsorption on bioactive glass

	Mean frequencies (cm ⁻¹)				
	α-helix	β-sheet	β-turn	random	aggregates
MnmE	1657.5	1624, 1639,1695	1680	-	-
MnmE on bioactive glass	1659	1638	1678	1648	1620

Furthermore, the peaks at 1624 and 1695 cm⁻¹ corresponding to β-sheets in the native structure of MnmE are significantly shifted after adsorption to 1620 and 1692.5 cm⁻¹, respectively, thus changing their assignment (Table 5). The 1620.0 cm⁻¹ component can instead be attributed to side chains and aggregates [ARRONDO and GONI 1999, SESHADRI *et al.* 1999], while the peak at about 1692 cm⁻¹ can be associated with β-turns [KONG and YU 2007, NATALELLO *et al.* 2005, SUSI and BYLER 1983].

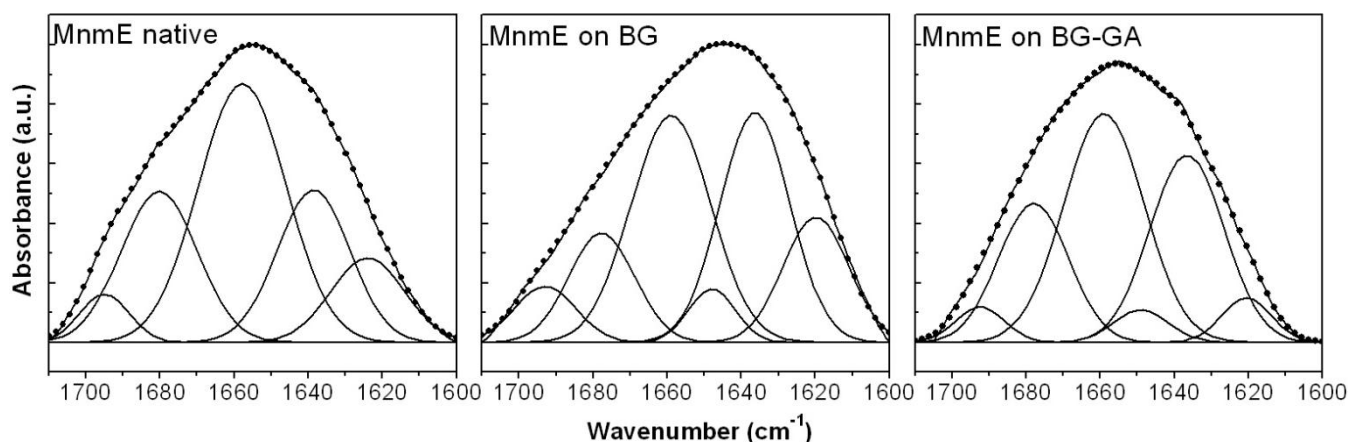
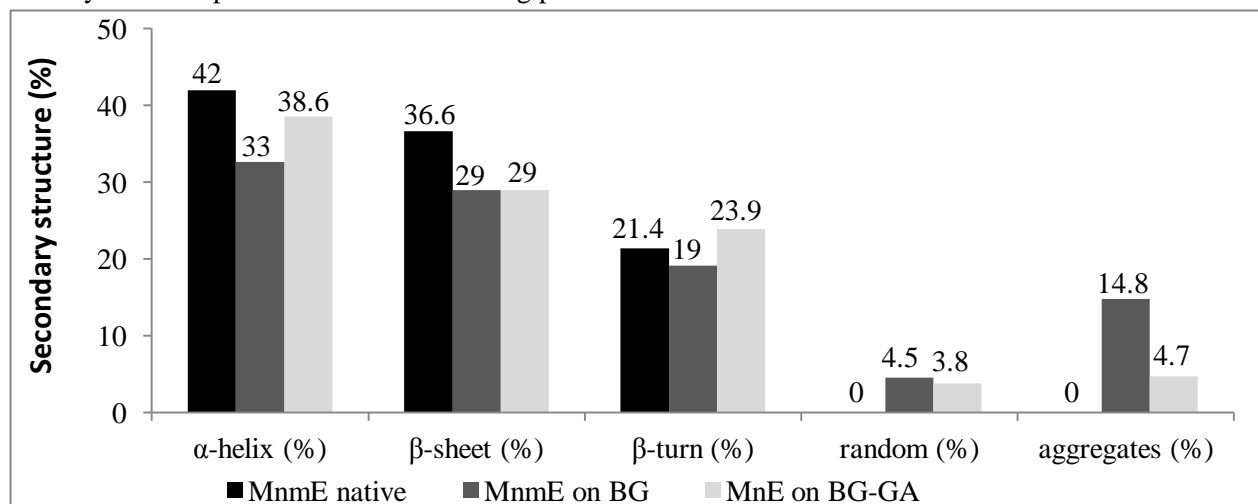


Figure 14 Separation of the amide I band into its components for MnME before and after adsorption on BG without and with GA. The closed circles represent the sum of the separated band components. The errors are ± 1 cm^{-1} for the band positions and $\pm 5\%$ for the peak areas.

Thereby, the general trend is that after adsorption the amount of α -helices and β -sheets decreases and less ordered structures (turns, random coils and aggregates) increase. These changes are less pronounced on the BG treated with GA (Table 6). It seems that the treatment with GA helps maintaining significantly larger amounts of α -helices in the MnME structure after adsorption although the loss in β -sheets percentage is the same as on the BG without GA. Moreover, the percentage of aggregates is much lower in case of BG treated with GA, indicating a lower degree of protein denaturation on this substrate (Table 6).

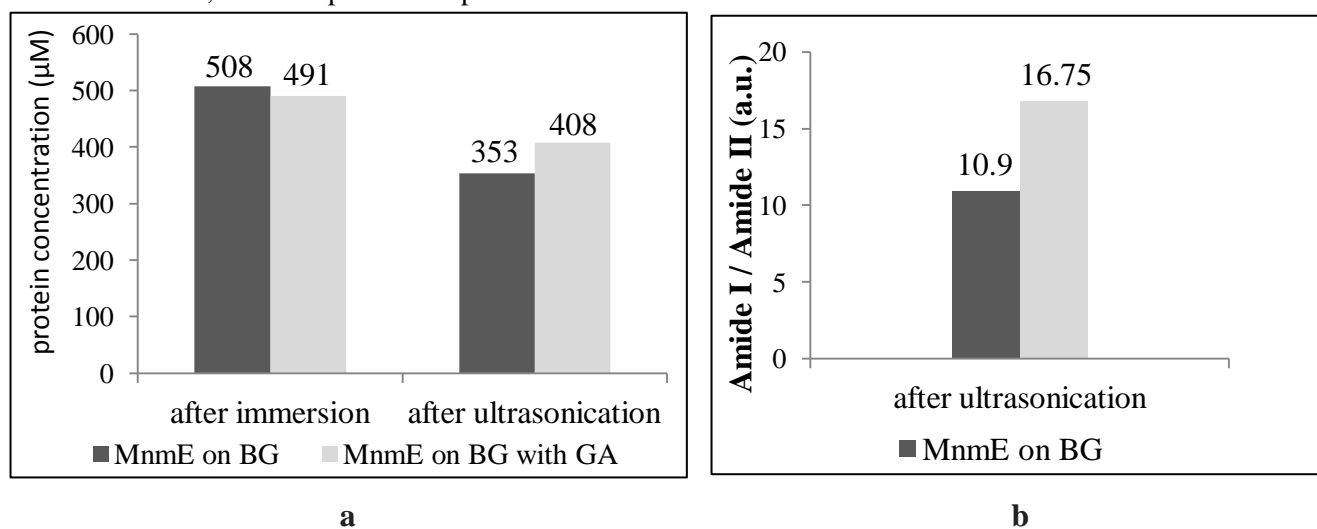
Table 6 Distribution of secondary structure elements in MnME before and after adsorption on BG. The uncertainty due to experimental error and fitting procedure are within the limit of $\pm 5\%$



3.2.4. Quantitative adsorption analysis

The amount of the protein attached on the bioactive glass was estimated from cw-EPR spectra recorded at room temperature. The values of protein concentration on both BG substrates are similar immediately after immersion, but the ultrasonication process removes more protein from the BG without GA, indicating stronger protein attachment on the surface treated with GA (Table 7a). These results are further supported by the values obtained from amide I/amide II ratio of FTIR spectra (Table 7b).

Table 7 (a) Molar concentration (in μM) of MnmE adsorbed on BG before and after ultrasonication. Errors are estimated to $\pm 10\%$, due to experimental settings and uncertainties in baseline subtraction. **(b)** Amide I/ Amide II ratio of intensities from FTIR spectra recorded for MnmE attached on BG after ultrasonication. Errors are estimated to $\pm 15\%$, due to experimental procedure and uncertainties in baseline subtraction.



The bioactive glass surface was further analyzed by means of X-ray photoelectron spectroscopy (XPS) before and after immersion in protein solution. The relative intensity of N 1s peak recorded at approximately 400 eV (Figure 15) was used to monitor the amount of protein attached on the BG surface (Table 8). As in the case of methemoglobin, the deconvolution of N 1s core level spectra recorded after adsorption has shown the presence of two components centered at 398.2 and 400 eV, the latest being typical for nitrogen in organic matrices [VANEVA and SIMON 2011, SERRO *et al.* 2006]. Like we expected, the BG treated with GA shows better protein coverage of the BG surface (Table 8), result which is consistent with results obtained by EPR and FTIR spectroscopy.

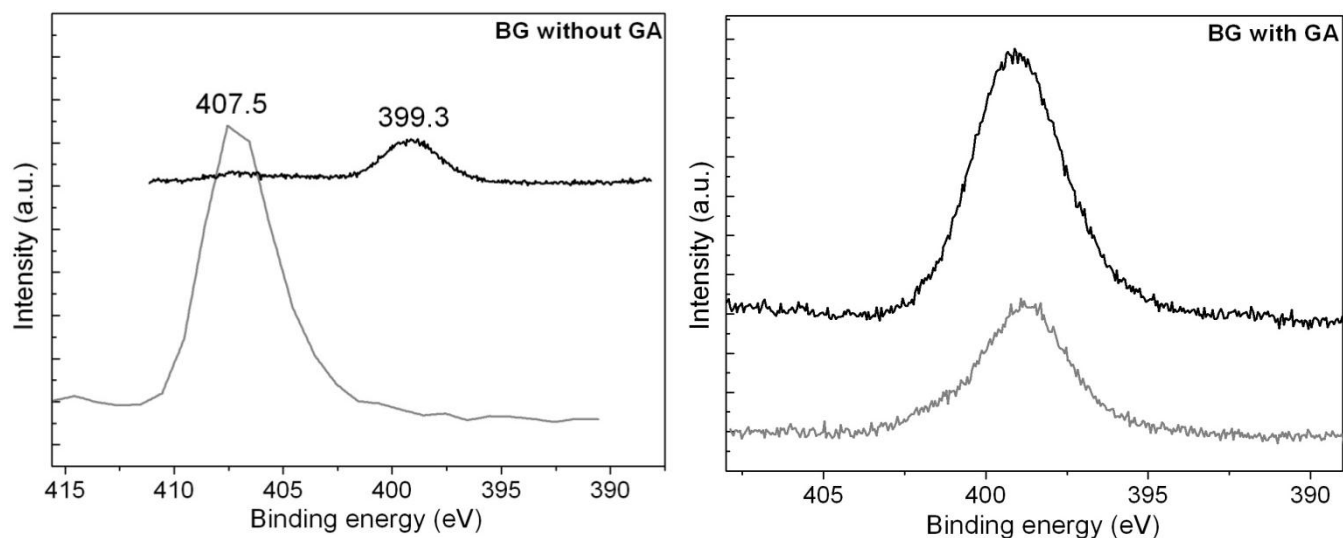
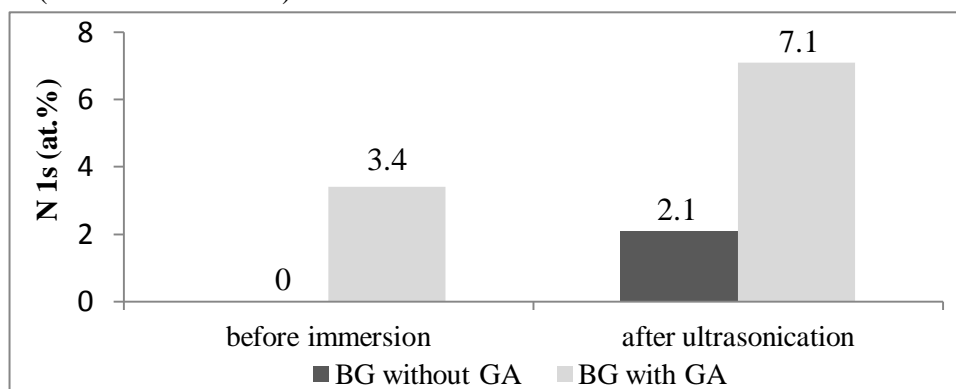


Figure 15 N 1s high resolution spectra of BG before (gray) and after immersion in MnME solution (black). The relative intensity of N 1s peak from ca. 400 eV was used to quantify protein attachment on the BG surface. (the N 1s peak recorded at 407.5 eV does not contain contributions associated to organic matrixes; therefore, a high resolution spectra was not needed in this situation, the peak was subtracted from survey spectrum of BG without GA)

Table 8 N1s atomic percentage on BG surface for the peak recorded at around 400 eV before and after immersion in MnME solution (after ultrasonication)



SEM images recorded on the BG surface before and after immersion in MnME solution show that after adsorption a uniform layer of protein covers the surface of both BG substrates (Figure 16 and Figure 17), but it can be easily seen that adsorption is influenced by glutaraldehyde. It seems as if the protein coupling agent leads to a better organization of the protein layer. Unlike the images for methemoglobin, the presence of protein chains is not visible here, confirming that polymerization of MnME is unlikely to occur. This assumption was already suggested by the results obtained by pulse DEER spectroscopy (see Section 3.2.2).

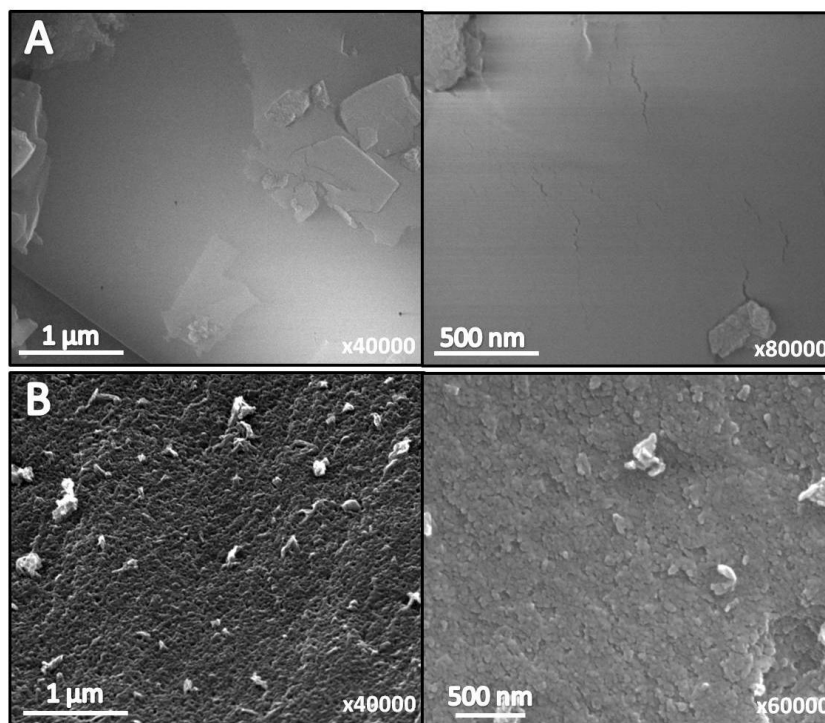


Figure 16 SEM images of BG without GA before (A) and after immersion in MnME solution (B). The images in the right are recorded with a higher magnification. After adsorption a uniform layer of protein covers the BG surface.

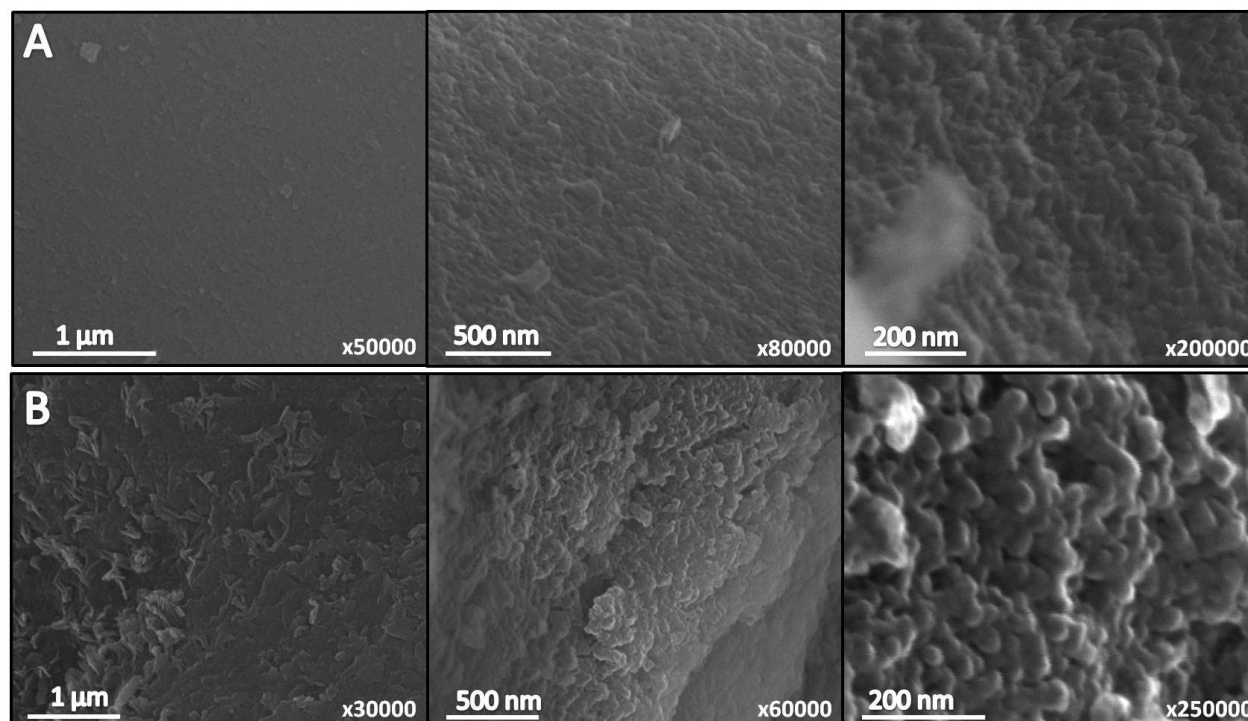


Figure 17 SEM images of the BG with GA, before (A) and after immersion in methemoglobin solution (B). The images in the center and right panels are recorded with higher magnification.

4. Conclusions

According to the first aim of this work, we have shown that EPR spectroscopy combined with site-directed spin labeling can be used to investigate adsorption of proteins on solid surfaces. For both proteins, X-band cw-EPR measurements revealed significant differences in the spin label mobility upon adsorption on bioactive glass, indicating that the movement of the entire protein molecule is restricted due to interaction with bioactive glass. Interestingly, for horse methemoglobin cw-EPR spectra recorded after adsorption revealed an increase in mobility of spin labels which are oriented towards the protein surface, suggesting a possible unfolding of the β -93 surroundings upon adsorption. Indeed, investigation of secondary structure of methemoglobin by FTIR spectroscopy confirmed that almost 20 % of the protein helical structure is unfolded after adsorption, while pulse DEER measurements have shown an increase of distance between the two positions β -93 after adsorption. According to results obtained by these three techniques we may conclude that the α -helix where position β -93 is located unfolds after adsorption.

In the case of MnmE, especially the two positions situated in the G-domain of the protein are affected by the interaction with the BG substrate, suggesting that the vicinities of positions E287 and S278 represent a contact point between the protein and the bioactive glass (see Figure 13). This assumption is further supported by the results obtained from pulse DEER spectroscopy that showed that the two G-domains remain in open state even after the addition of GDP·AlF_x, as a consequence of immobilization of the G-domains on the BG surface.

One of the most important conclusions of this study is the assumption that both proteins dissociate upon adsorption on the bioactive glass. This hypothesis is corroborated by the low modulation depth of all DEER time traces recorded after adsorption. In fact, in the case of MnmE the modulation depth was reduced almost completely so that it was impossible to obtain a distance distribution. This result leads us to the conclusion that the functionality of MnmE is drastically affected upon adsorption. However, this issue is not of crucial importance in evaluating the biocompatibility of a biomaterial. Previous studies have shown that the effect of adsorbed protein on cell attachment is highly dependent on the quantity of the protein attached [XIE *et al.* 2001, ZENG *et al.* 1999] and orientation of the protein molecule on the surface of the biomaterial [BUCHANAN and EL-GHANNAM 2010, CHITTUR 1998]. Moreover, it was recently demonstrated that a protein conformation rich in flexible and charged unordered structure enhances the success of cell attachment and spreading on the surface of bioactive glass [BUCHANAN and EL-GHANNAM 2010].

Another aim of this study was to investigate the effect of glutaraldehyde in protein attachment. In this respect, the surface of bioactive glass was silanized with 3-aminopropyl-triethoxysilane and then functionalized with glutaraldehyde. Quantitative analyses have shown that for both proteins glutaraldehyde positively influences the binding stability on bioactive glass. It seems that the presence of GA offers more stable and specific points for protein attachment on the BG substrate, so the binding and distribution of the protein might be more organized as compared to untreated BG. If the BG substrate is not functionalized with GA, the protein covers every accessible place on the surface with some protein molecules having only weak attachment points so they can easily detach when the sample is ultrasonicated. This hypothesis is highlighted by SEM characterization of the bioactive glass surface before and after immersion in protein solutions.

Regarding the effect of glutaraldehyde in maintenance of protein native structure upon adsorption, investigations performed by FTIR spectroscopy have shown that indeed for both proteins a higher percentage of α -helical structure remains intact after adsorption. On the level of tertiary structure, pulse DEER measurements revealed that only on the bioactive glass functionalized with GA a small amount from the protein attached is able to preserve its dimeric structure. These results confirm that the protein coupling agent plays a role in maintaining the native structure of both proteins upon adsorption but the effect on tertiary structure is much weaker than on secondary structure elements. Methemoglobin represents a special case, because it was already shown that hemoglobin polymerizes in the presence of glutaraldehyde [MacDONALD and PEPPER 1994, GUILLOCHON *et al.* 1986, WEETALL 1974]. Accordingly, zero modulation depth of the DEER signal confirmed that treatment of BG surface with glutaraldehyde induces polymerization of methemoglobin upon adsorption. Moreover, images obtained by means of scanning electron microscopy revealed that glutaraldehyde leads to the cross-linking of methemoglobin [WEETALL 1974], resulting in formation of macromolecules consisting of 8-10 proteins.

All the results presented above prove that EPR in combination with site-directed spin labeling is a powerful tool for studying protein structure and dynamics after adsorption on solid substrates. The main advantage of this method is that proteins can be investigated in their native environment, allowing thus to obtain information about protein dynamics and functionality not only in solution but also in adsorbed state. Moreover, investigations with three different techniques certified that EPR spectroscopy can be used to quantify the protein attached on a solid substrate. This kind of information is of crucial importance in the field of biomaterials and helps in understanding protein behavior upon interaction with solid environments.

SELECTIVE BIBLIOGRAPHY

1. [ANTONINI and BRUNORI 1971] Antonini E and Brunori M in *Myoglobin and Hemoglobin in their Reactions with Ligands*, eds. Neuberger, A. & Tatum, EL (North-Holland, Amsterdam), Vol. 21. (1971).
2. [ARRONDO and GONI 1999] Arrondo JLR and Goni FM, *Prog. Biophys. Mol. Biol.* 72 (1999) 367–405.
3. [BANHAM *et al.* 2007] Banham JE, Jeschke G, Timmel CR, *Molecular Physics* 105 (2007) 2041-47.
4. [BOEHME 2010] Boehme S, *Structural and functional analysis of the MnmE/ Gid A protein complex studied by EPR spectroscopy*, 2010. Department of Biology, University of Osnabrueck, Germany. Ref Type: Thesis/Dissertation.
5. [BOEHME *et al.* 2010a] Böhme Sabine, Simon Meyer, André Krüger, Heinz-Jürgen Steinhoff, Alfred Wittinghofer, Johann P. Klare, *J. Biol. Chem.*, 285 (2010) 16991-17000.
6. [BOEHME *et al.* 2010b] Sabine Böhme, Heinz-Jürgen Steinhoff and Johann P. Klare, *Spectroscopy*, 2010, 24 (3-4), 283-288
7. [BORDIGNON and STEINHOFF 2007] Bordignon E, Steinhoff HJ, *Membrane protein structure and dynamics studied by side-directed spin labeling ESR*, in: Hemminga MA, Berliner LJ (Eds), *ESR Spectroscopy in Membrane Biophysics*, Springer Science and Business Media, New York, 2007, pp. 129-164.
8. [BRIDGES *et al.* 2010] Bridges MD, Hideg K, Hubbell WL, *Appl Magn Reson* 37 (2010) 363–390.
9. [BROWNE *et al.* 2004] Browne MM, Lubarsky GV, Davidson MR, Bradley RH, *Surf. Sci.* 553 (2004) 155–167.
10. [BUCHANAN and EL-GHANNAM 2010] Buchanan LA, El-Ghannam A, *J. Biomed. Mater. Res. A* 93 (2010) 537-546.
11. [BYLER and SUSI 1986] Byler DM and Susi H, *Biopolymer* 25 (1986) 469–487.
12. [CAI and SINGH 2004] Cai S and Singh BR, *Biochemistry* 43 (2004) 2541-2549.
13. [CHEN *et al.* 2006] Chen QZ, Rezwan K, Armitage D, Nazhat SN, Boccaccini AR, *J. Mater. Sci.: Mater. Med.* 17 (2006) 979-87.
14. [CHEN *et al.* 2007] Chen QZ, Rezwan K, Françon V, Armitage D, Nazhat SN, Jones FH, Boccaccini AR, *Acta Biomaterialia* 3 (2007) 551-62.
15. [CHITTUR 1998] Chittur K, *Biomaterials* 19 (1998) 357–369.
16. [DONG *et al.* 1994] Dong A, Caughey WS, Du Clos TW, *J. Biol. Chem.* 269 (9) (1994) 6424–6430.
17. [DOUSSEAU and PEZOLET 1990] Dousseau F, Pezolet M, *Biochemistry* 29 (1990) 8771-8779.
18. [EL-GHANNAM *et al.* 1999] El-Ghannam A, Ducheyne P, Shapiro IM, *J. Orthop. Res.* 17 (1999) 340-345.
19. [FANUCCI *et al.* 2003] Fanucci GE, Cogshall KA, Cadieux N, Kim M, Kadner RJ, Cafiso DS, *Biochemistry* 2003, 42, 1391.
20. [GASPER *et al.* 2009] Gasper R, Meyer S, Gotthardt K, Sirajuddin M, and Wittinghofer A, *Nat. Rev. Mol. Cell Biol.* 10 (2009) 423–429
21. [GRAY 2004] Gray JJ, *Current Opinion in Structural Biology* 14 (2004) 110–115.

22. [GRUIAN *et al.* 2011a] Gruian C, Steinhoff HJ, Simon S, Digest Journal of Nanomaterials and Biostructures 6 (2011) 373-83.
23. [GRUIAN *et al.* 2011b] Gruian C, Steinhoff HJ, Simon S, Studia Chemia 2 (2011) (accepted)
24. [GUILLOCHON *et al.* 1986] Guillochon D, Vijayakshmi M W, Thiam-Sow A, Thomas D, Biochem. and Cell. Biol. 64 (1986) 29-37.
25. [HENCH and WEST 1990] Hench LL, West JK, Chem Rev 90 (1990) 33-72.
26. [HEULE *et al.* 2003] Heule M, Rezwani K, Cavalli L, Gauckler LJ, Advanced Materials. 15 (2003) 1191–1194.
27. [HUBBELL *et al.* 2000] Hubbell WL, Cafiso DS, Altenbach C, Nat. Struct. Biol. 2000, 7, 735.
28. [JACOBSEN *et al.* 2005] Jacobsen K, Oga S, Hubbell WL, Risse T, Biophys. J. 88 (2005) 4351-4365.
29. [JACOBSEN *et al.* 2006] Jacobsen K, Hubbell WL, Ernst OP, Risse T, Angew. Chem. Int. Ed., 45 (2006) 3874-3877.
30. [JESCHKE *et al.* 2006] Jeschke G, Chechik V, Ionita P, Godt A, Zimmermann H, Banham J, Timmel CR, Hilger D, Jung H, Appl Magn Reson, 30 (2006) 473-498
31. [KARLSSON *et al.* 2000] Karlsson M, Martensson LG, Jonsson BH, Carlsson U, Langmuir 2000, 16, 8470.
32. [KLARE and STEINHOFF 2009] Klare JP, Steinhoff HJ, Photosynth Res. 102 (2009) 377-90.
33. [KONG and YU 2007] Kong J and Yu S, Acta Biochimica et Biophysica Sinica 39 (2007) 549–559.
34. [LATOUR 2005] Latour RA Jr., *Biomaterials: Protein-Surface Interactions*, in: Taylor & Francis (Eds) Encyclopedia of Biomaterials and Biomedical Engineering, Informa Healthcare, New York 2005, pp.1-15.
35. [LUO *et al.* 1994] Luo S, Huang CYF, McClelland JF, Graves DJ, Analytical Biochemistry 216 (1994) 67-76.
36. [MACDONALD and PEPPER 1994] MacDonald SL, Pepper DS, Methods Enzymol. 231 (1994) 287-308.
37. [MCCALLEY *et al.* 1972] McCalley RC, Shimshick EJ, McConell HM, Chem. Phys. Lett. 13 (1972) 115-119
38. [MEYER *et al.* 2009] Meyer S, Böhme S, Krüger A, Steinhoff HJ, Klare JP, Wittinghofer A, PLoS Biology 7 (2009) e1000212.
39. [MOFFAT 1971] Moffat JK, J. Mol. Biol. 55 (1971) 135-46.
40. [MUIR *et al.* 2008] Muir BW, Tarasova A, Gengenbach TR, Menzies DJ, Meagher L, Rovere F, Fairbrother A, McLean KM, Hartley PG, Langmuir 24 (2008) 3828–3835.
41. [NATALELLO *et al.* 2005] Natalello A, Ami D, Brocca S, Lotti M, Doglia SM, Biochem. J 385 (2005) 511–517.
42. [OKUDA *et al.* 1991] Okuda K, Urabe I, Yamada Y, Okada H, J. Ferment. Bioeng. 71 (1991) 100-5.
43. [PANNIER *et al.* 2000] Pannier M, Veit S, Godt A, Jeschke G, Spiess HW, Journal of Magnetic Resonance 142 (2000) 331–340.
44. [PIN and ROYER 1994] Pin S and Royer CA, Methods Enzymol. 232 (1994) 42–55.
45. [POLYHACH and JESCHKE 2007] Polyhach Ye, Jeschke G, Physical Chemistry Chemical Physics, 9 (2007) 1895–1910.

46. [RISSE *et al.* 2003] Risse T, Hubbell WL, Isas JM, Haigler HT, Phys. Rev. Lett. 91 (2003) 188101-188105.
47. [SCRIMA *et al.* 2005] Scrima A, Vetter IR, Armengod ME, Wittinghofer A, EMBO J, 24 (2005) 23-33.
48. [SCRIMA and WITTINGHOFER 2006] Scrima A and Wittinghofer A, EMBO J, 25 (2006) 2940-2951.
49. [SERRO *et al.* 2006] Serro AP, Gispert MP, Martins MCL, Brogueira P, Colaco R, Saramago B, Biomed. Mater. Res. 78A (2006) 581–589.
50. [SERVAGENT-NOINVILLE *et al.* 2000] Servagent-Noinville S, Revault M, Quiquampoix H, Baron M, J. Colloid. Interface Sci. 221 (2000) 273-283.
51. [SESHADRI *et al.* 1999] Seshadri S, Khurana R, Fink AL, Methods Enzymol 309 (1999) 559–576.
52. [STEINHOFF *et al.* 1989] Steinhoff HJ, Lieutenant K, Redhardt A, Biochimica et Biophysica Acta 996 (1989) 49-56.
53. [SUSI and BYLER 1983] Susi H and Byler DM, Biochemical and Biophysical Research Communications, 115 (1983) 391-397.
54. [TIAN *et al.* 1998] Tian MH, Lee WK, Bothwell MK, McGuire J, J. Colloid Interface Sci. 1998, 200, 146.
55. [TUNC *et al.* 2005] Tunc S, Maitz MF, Steiner G, Vazquez L, Pham MT, Salzer R, Colloids and Surfaces B: Biointerfaces 42 (2005) 219–225.
56. [VALDES and ACKERS 1977] Valdes RJ and Ackers GK, J. Biol. Chem. 252, (1977) 74–81.
57. [VANEVA and SIMON 2011] Vanea E and Simon V, Applied Surface Science 257 (2011) 2346–2352
58. [VERNE *et al.* 2009] Verne E, Vitale-Brovarone C, Bui E, Bianchi CL, Boccaccini AR, Journal of Biomedical Materials Research Part A 90 (2009) 981-992.
61. [WEETALL 1974] Weetall HH, Anal. Chem. 46 (1974) 602-615a.
62. [WEETALL 1985] Weetall HH, Trends Biotechnol. 3 (1985) 276-280.
63. [WERTZ and SANTORE 2001] Wertz CF, Santore MM, Langmuir 17 (2001) 3006-3016.
64. [WILLIAMS and BLANCH 1994] Williams RA, Blanch HW, Biosens. Bioelectron. 9 (1994) 159-167.
59. [XIE *et al.* 2001] Xie J, Riley C, Chittur K, J Biomed Mater Res 57 (2001) 357–365.
60. [ZENG *et al.* 1999] Zeng H, Chittur KK, Lacefield WR, Biomaterials 20 (1999) 377–384.